University of Stavanger

University of Stavanger

Faculty of Science and Technology

MASTER'S THESIS

Study program/ Specialization: Msc Petroleum Geosciences Engineering	Spring semester, 2014 Open / Restricted access
Writer: Torbjørn Ladstein Fjeld	…… (Writer's signature)
Faculty supervisor: Alejandro Escalona External supervisor(s):	
Thesis title: Seismic Characterization of Lower Cretaceous clastic wedges in the Tromsø Basin	
Credits (ECTS): 30	
Key words: Barents Sea Lower Cretaceous Clastic wedges Syn-rift Knurr Formation Seismic facies	Pages: …… + enclosure: …… Stavanger, …….. Date/year

Copyright

by

Torbjørn Ladstein Fjeld

2014

University of Stavanger

Seismic Characterization of Lower Cretaceous clastic wedges in the Tromsø Basin

by

Torbjørn Ladstein Fjeld, Bsc Petroleum Geology

Msc Thesis

Presented to the Faculty of Science and Technology

The University of Stavanger

The University of Stavanger

June 2014

University of Stavanger

ACKNOWLEDGEMENTS

The following are acknowledged for their help and support during the research and writing of this thesis.

Firstly I would like to thank my supervisor Alejandro Escalona, for his support and feedback throughout the work and writing process.

Thanks to Phd candidate Dora Marin for help and support throughout this work.

Thanks to my family and friends for their support.

Thanks to the LoCrA consortium for the founding of the project.

University of Stavanger

Abstract

Seismic Characterization of Lower Cretaceous clastic wedges in the Tromsø Basin

Torbjørn Ladstein Fjeld, Bsc Petroleum Geology

The University of Stavanger, 2014

Supervisor: Alejandro Escalona

In this study, seismic reflection, well logs and core data has been used to characterize Lower Cretaceous marine to deep marine syn-rift clastic wedges in the southwestern Barents Sea. The study area is situated on a faulted terrace towards the Tromsø Basin away from the Finnmark Platform. The terrace is confined an intersection between three major fault zones which confines the structure. The structure is heavily segmented, generating sub-terraces and along strike depocenters towards the Tromsø Basin. Three main fault families are controlling the paleodrainage, in which two are controlling the sediment dispersal into the structure and one is controlling the distribution of sediments. Seismic characterization reveals three seismic facies, from chaotic low amplitude to continuous high amplitude reflections. Characterization from the seismic reveals several depositional environments, in which one of the seismic facies penetrated and controlled by well data. Three main lithofacies have been distinguished in core, and consists of heterolithic mudstones, debris flows and high density turbidites.

University of Stavanger

Contents

INTRODUCTION 1
Objective and motivation 2
REGIONAL SETTING 6
Geologic setting of the Tromsø Basin 6
Stratigraphy 7
Theoretical background on rift basins 15
The evolution of normal faults 15
DATABASE AND METHODS 20
Seismic Data and Well Data 20
Data quality 20
Study Methods 21
OBSERVATIONS 25
Well and core description of well 7019/1-1 25
Structural interpretation 29
Structural configuration of surfaces 30
Seismic Characterization 37
Seismic Facies 37
DISCUSSION 46
Footwall uplift and control on paleodrainage 46
Structural Evolution of FF2 46
Evolution of Lower Cretaceous wedges in the TFFC 47
Seismic facies and grain size distribution vs. slope gradients 51
Petroleum potential 52
Field analogues 52
Reservoir potential 52
Seismic resolution and limitations 55
CONCLUSIONS 56
REFERENCES 57
Appendix 59

University of Stavanger

List of figures

Fig. 1, Structural map of the Norwegian Barents Sea. Red box is indicating the study area, with the location of discovery well 7019/1-1. A-A' gives the location of Fig.2. White dots: wells that penetrated Lower Cretaceous. Yellow dots: Technical discoveries with Lower Cretaceous as primary and/or secondary target. Red dots: Dry wells with Lower Cretaceous as primary and/or secondary target. Blue dots: Wells that does not penetrate Lower Cretaceous (generally situated on platforms and basement highs e.g., Loppa High and Finnmark Platform, areas where large amount of Mesozoic is eroded). Green dots: Planned and active exploration wells (summer 2014). The structural map is modified from www.npd.no. Well data compiled by Grundvåg et al. (2014) 4
Fig. 2, Crossline A-A' across the Hammerfest Basin, indicating that clastic wedges are developed along the margins of the basi,n sourced from the uplifted Loppa High and Finnmark Platform. Targeted wells are both dry and with shows Seldal (2005). Location of line in fig. 1 4
Fig. 3, Pressure vs. depth cross-plot showing the differences in pressure between the Lower Cretaceous and the Middle Jurassic reservoirs in well 7019/1-1 (left column, red dots) Halland et al. (2014). 5
Fig. 4, Combined Gravity map and main structural elements in the study area. 9
Fig. 5, Summarized plate model, illustrating the plate movements from Late Jurassic to present. From A-B Greenland is rotating, genereating the Early Cretaceous rift structures.C), the initial opening of the North Atlantic. D) Present day plate geometry of the North Atlantic and Barents Sea. The plate model is constructed in PaleoGis from the plate model provided by the Plates team at the University of Texas Institute for Geophysics. 10
Fig. 6, Litostratrigraphic column correlated with synthetic and gamma ray of well 7019/1-1, and a summary of the main tectonic events for late Mesozoic and Cenozoic. Composed from (Gradstein et al., 2010; Smelror et al., 2009) 11
Fig. 7, Interpreted and uninterpreted regional seismic line TR-73R1-711. A'—A crossing the Finnmark Platoform into the Hammerfest Basin towards the Ringvassøy Loppa Fault Complex, into the Tromsø basin and towards the Senja Ridge to in the west.. Upper Right: Base Cretaceus Unconformity map with location of the line. 13
Fig. 8, Interpreted and uninterpreted regional seismic line T-01-84. B'—B is crossing the study area illustrating how the Lower Cretaceous fault have more listric geometries and are being offset by a younger fault towards the Tromsø Basin. The southern elongation of the Senja Ridge is located deeper into the Tromsø Basin. Location of line top right. 14
Fig. 9, Schematic evolution of three segments, following the three stages of fault evolution, with displacements profiles. Notice how the displacement profile in stage C) is similar to the displacement profile of fault A in stage A). (Gawthorpe and Leeder, 2000) 16
Fig. 10: Block diagrams illustrating the evolution of the three stages. Notice how faults like Y and Z forms during the initiation stage, but later become inactive. (Gawthorpe and Leeder, 2000) 17
Fig. 11, Block diagram with grid indication how the internal relief of half grabens will control the sediment dispersal. A-A' shows a cross section through a half graben, indication how the flexural footwall uplift will form a drainage divide in which sediment dispersal shifts away from the fault. Syn-rift sediments are forming a syn-tectonic wedge towards the adjacent fault. RR: Relay ramp. Modified from Ravnas and Steel (1998) 18
Fig. 12, idealized illustration of depositional environments of marine to deep-marine rift basins (left to right). Several processes of drainage are involved, orthogonal deposition sourced from adjacent faults and axial deposition into relay zones and along the faults. (Ravnas and Steel, 1998) 19

Fig. 13, Seismic and well database map. 22
Fig. 14, Amplitude vs. Frequency plot of three surveys in the dataset used in this study. Especially the low frequency bandwidth of the 3D survey (green line) indicates that the 3D has low vertical resolution 23
Fig. 15, Comparison of the vertical resolution of the seismic surveys. Illustrating the low frequency of the 3D compared to the 2D data. The 3D line has a random direction to mimic the navigation of T-014-85 (from NPD-TR-85 Fig. 16). 24
Fig. 16, Well 7019/1-1 lithological column of the core, correlated with gamma ray, density-neutron and ressistivity logs. Black bar indicate the interval of the core. 28
Fig. 17, Base Cretaceous Unconformity time structural map, with main faults families and locations of N-S tie line (Fig. 18), and diplines A-F (Fig. 19, 20). 1: Breached relay. 2: Relay ramp. 3: Horst. 4:Graben. 5: Half-graben. 31
Fig. 18, N-S seismic random well tie line. Showing main horizons interpreted, and the structural deformation styles of the area crossing FF1 and FF2. Location of line is shown in figure 17. 32
Fig. 19, Diplines A-C showing how the segmented structure is changing along strike. Blue line: Top of Stø Formation, Red line: BCU, Green line: Top of Knurr Formation. 33
Fig. 20, Diplines D-F showing how the segmented structure is changing along strike. Blue line: Top of Stø Formation, Red line: BCU, Green line: Top of Knurr Formation. Note that lines E and F are 2D lines and have a smaller scale than the previous four lines from the 3D. 34
Fig. 21, Time structural map of the Top of Stø Formation, with the navigation of diplines A-F (Fig. 19, 20). 35
Fig. 22, Time structural map of the Top of Knurr Formation. 36
Fig. 23, Seismic 2D line TGS-90-202 along the strike of the wedge. Illustrating how the Lower Cretaceous wedge is filling and spilling towards north. Location of well 7019/1-1 is projected into the line. 40
Fig. 24, closer look of the southern section of TGS-90-202, highlighting the identified seismic facies. Chaotic architecture of SF2 filling on top of BCU. SF3 is filling and spilling towards north. Navigation of Fig. 25 indicated by black vertical line. 41
Fig. 25, Interpreted and uninterpreted dipline T-013-85, across the structure. SF1b is localized adjacent to a major fault. SF2 and SF3 are confined into a narrow graben onlapping BCU. Truncations of pre-rift Jurassic reflectors are indicating footwall erosion. SF2 may be sourced orthogonal from the adjacent footwall to the SE and the uplifted horst to the NW. SF3 is onlapping SF2 and BCU. 42
Fig. 26, Seismic facies maps illustrating the distribution of seismic facies, and their respective areal extent recognized in this study, ...43
Fig. 27, Time thickness map of the Lower Cretaceous wedge (BCU-Top Knurr). Showing that the wedges are preserved as elongated bodies along the main rift axis, and are thickening towards the basin bounding faults. 44
Fig. 28, Seismic attribute map, RMS. Minor anomalies of the attributes indicate thicker packages of the syn-rift. 45
Fig. 29, 3D overview of the structure. Looking towards east, the coastline of Finnmark is in the top right. The structure is projected by the base Cretaceous unconformity with the well location in the north. On the Finnmark Platform ,a map of the seafloor is projected, representing the unconformity at the Finnmark platform, as the BCU is eroded. The three main fault families are indicated by arrows. Notice how the structure gets deeper towards the north. 48

Fig. 30, Proposed map of the paleodrainage of the syn-rift succession during Lower Cretaceous. The flexural footwall uplift of the three main faults will confine the catchment area for preserving the sediments. The structure has a relief towards northwest. 49
Fig. 31, Conceptual model, illustrating the syn-tectonic depositional processes proposed during Lower Cretaceous in the study area. Identified seismic facies is annotated in the figure. Modified from (Ravnas and Steel, 1998) 50
Fig. 32, Slope gradients calculated from Line TGS-90-202, showing the relief of the drainage towards the well location in the north, location of line in fig.23. 51
Fig. 33 Britannia Field UK, A: Location of the Britannia Field in the Moray Firth Basin offshore UK in the North Sea. B: Size of the Britannia Field, with hydrocarbon contacts. C: Arrows are indicating several sources of sedimentation and paleodrainage. D: Samples of typical lithofacies found in the Britannia Field. (Copestake et al., 2003) 53
Fig. 34, Wells from the Britannia Field, illustrating how the turbiditic sands are pinching out from proximal to distal. If well 7019/1-1 is situated in a distal part of a turbiditic system, there remains a large potential for better reservoirs proximal. (Copestake et al., 2003) 53
Fig. 35, Size comparison of the Britannia Field compared to the study area. 54
Fig. 36, Porosity vs. depth chart from Henriksen et al. (2011), comparing present day burial (top) and maximum burial depth (bottom). The core porosity data points in well 7019/1-1 are calculated in the Jurassic sandstones. 54

List of Tables

Table 1, description, interpretation and examples of the main lithofacies identified in the Knurr Formation in well 7019/1-1. 28
Table 2, Summary of observations of main seismic facies identified in this study. 39

List of Appendix

Appendix 1, complete list of seimsic surveys/lines used in this study. 60
Appendix 2, complete image of the cored interval of the Knurr Formation in well 7019/1-1. Top of core (2220.0m TVD) is top left, bottom of the core (2234.3m TVD) is bottom right. Parts of the core is missing due to seal peal or sampling.....61
Appendix 3, complete lithological log of core 1, 7019/1-1 with comments.....62

INTRODUCTION

The Arctic is one of the remaining frontier petroleum provinces in the world. The exploration history of the Norwegian Barents Sea started back in the early 1980s, and as of today only around 80 exploration wells have been drilled. One producing field (Snøhvit) has been put in production. With the recent discoveries (Johan Castberg(2011), Norvarg(2011) and Gohta(2013), Wisting(2013)), the province has received renewed attention, and companies are testing several play models. The province has a total of 27 play models, NPD (2013), of which the Lower Cretaceous are clastic wedges in the west and clinoform targets in the east. The most prolific areas for exploration have generally been in the Hammerfest Basin and western parts of the Loppa High (Fig. 1), where the most successful play have been Jurassic and Triassic reservoirs. Through drilling campaigns of these plays, several exploration wells have penetrated Lower Cretaceous clastic wedges with good reservoir qualities (Fig. 1) (e.g., 7122/2-1, 7120/1-2, 7120/10-1). In particular these wedges seem to be better developed along the margins of the Hammerfest Basin towards the Finnmark Platform and along the southern part of the Loppa High (Fig. 2). Several of these wedges, contain hydrocarbons, mostly gas and oil shows. As of today, there are no commercial discoveries in the Lower Cretaceous, though estimates for undiscovered resources shows a large potential NPD (2013).

Exploration well 7019/1-1, drilled by Norsk Agip in 2000, has as a primary target the Middle Jurassic Stø Formation, with the Lower Cretaceous Knurr Formation as a secondary target. The well encountered gas in both targets, and is considered as a technical discovery for both. According to Halland et al. (2014); Seldal (2005), it contained more than 50% $C0_2$ in the Jurassic and less than 15% in the Lower Cretaceous. The much lower $C0_2$ content in the Lower Cretaceous indicates a barrier between the two reservoirs supported by the pressure plot between them (Fig. 3). Seldal (2005), states that oil shows were found in the top and bottom of the Lower Cretaceous Knurr Formation. As the well drilled into Jurassic shales prior to finding any contacts below the gas, it could indicate a gas oil contact downdip in the structure, south of the well location. 52m of net sandstone was encountered in the Knurr Formation, with an average porosity of 13% and a net/gross of 0.42. The dating of the Knurr Formation in the well was found to be Valangian to Barremian.

Active tectonic activity during Lower Cretaceous has developed gravity deposits across the Barents Sea basins (locra.ux.uis.no/proposal.pdf). Time equivalent gravity deposits to the Knurr Formation are encountered on Svalbard in the Rurikfjellet Formation (Grundvåg

and Olaussen, 2013) and eastern Greenland (Surlyk, 1984). Seldal (2005) describes the potential that exist in the Lower Cretaceous clastic wedges, and highlight the presence of hydrocarbons shows in almost all wells that have encountered reservoirs in Lower Cretaceous in the Barents Sea. As of today few published studies have focused on the Lower Cretaceous clastic wedges, and there is consequently little understanding on the mechanism for deposition, distribution and lack of detailed internal description of the wedges.

Objective and motivation

As a part of the LoCrA project (locra.ux.uis.no) this study focuses on the investigation and characterization of Lower Cretaceous clastic wedges penetrated in well 7019/1-1 towards the Tromsø Basin, by using well and seismic data. The objective is to develop a more detailed understanding of the depositional environments, syn-rift evolution, depositional processes, and the internal geometries of the wedges, in order to make a more detailed understanding of the paleodrainage and the structural control on deposition. This may to help improve the potential for petroleum exploration with a better prediction of reservoir and their lateral variability, and an understanding of trapping mechanisms related to the stratigraphic pinch out of these sandstones.

University of Stavanger

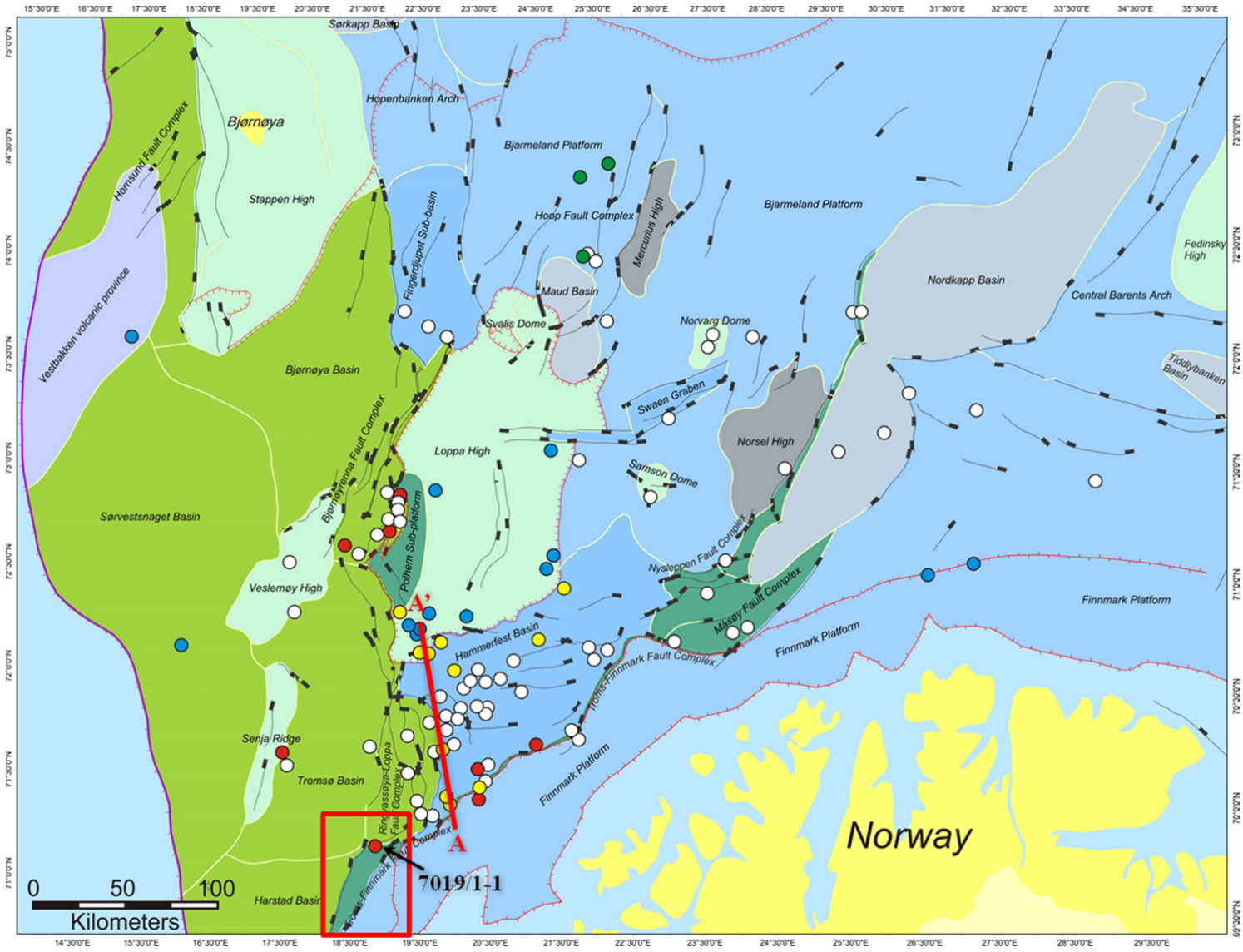

Fig. 1, Structural map of the Norwegian Barents Sea. Red box is indicating the study area, with the location of discovery well 7019/1-1. A-A' gives the location of Fig.2. White dots: wells that penetrated Lower Cretaceous. Yellow dots: Technical discoveries with Lower Cretaceous as primary and/or secondary target. Red dots: Dry wells with Lower Cretaceous as primary and/or secondary target. Blue dots: Wells that does not penetrate Lower Cretaceous (generally situated on platforms and basement highs e.g., Loppa High and Finnmark Platform, areas where large amount of Mesozoic is eroded). Green dots: Planned and active exploration wells (summer 2014). The structural map is modified from www.npd.no. Well data compiled by Grundvåg et al. (2014)

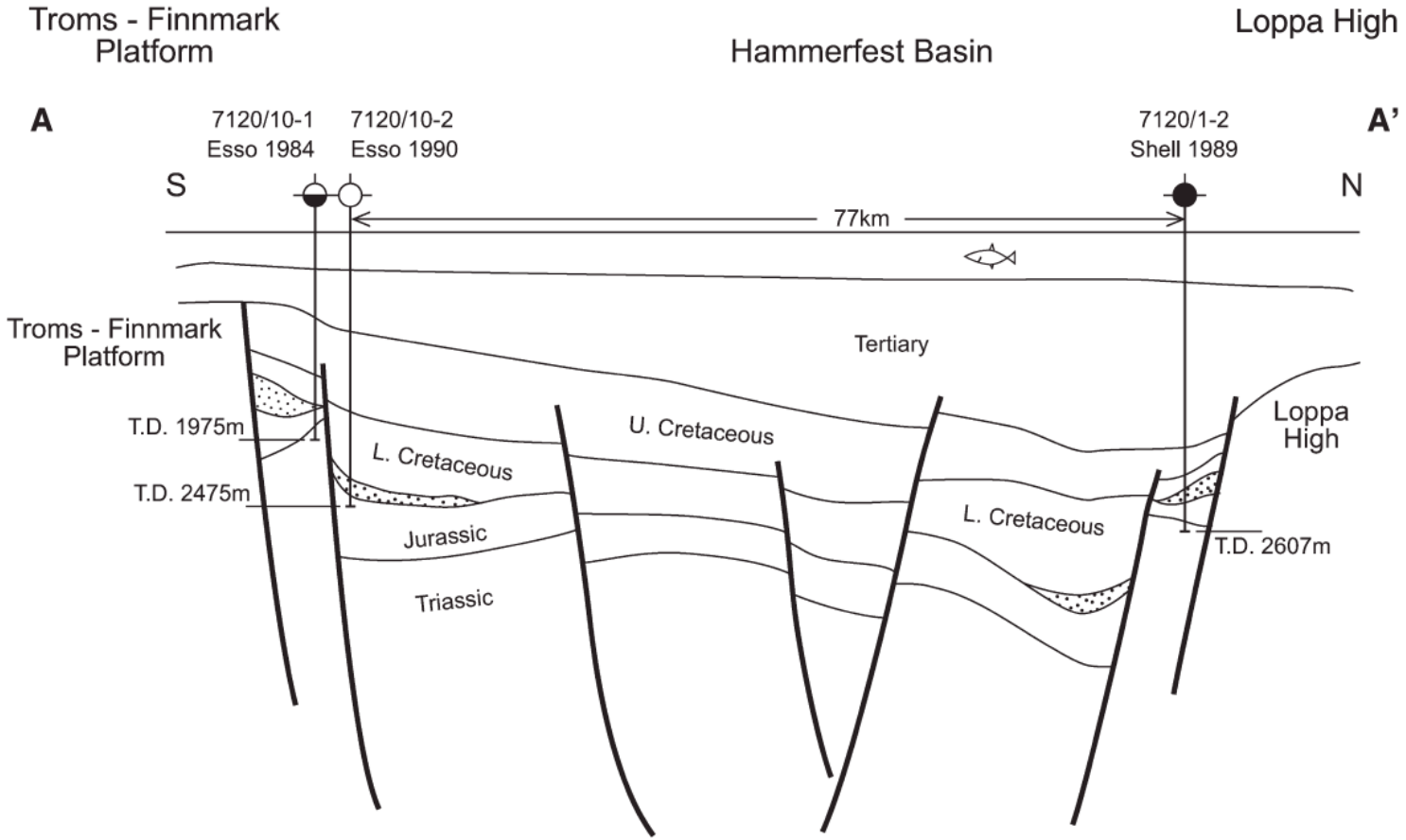

Fig. 2, Crossline A-A' across the Hammerfest Basin, indicating that clastic wedges are developed along the margins of the basi,n sourced from the uplifted Loppa High and Finnmark Platform. Targeted wells are both dry and with shows Seldal (2005). Location of line in fig. 1

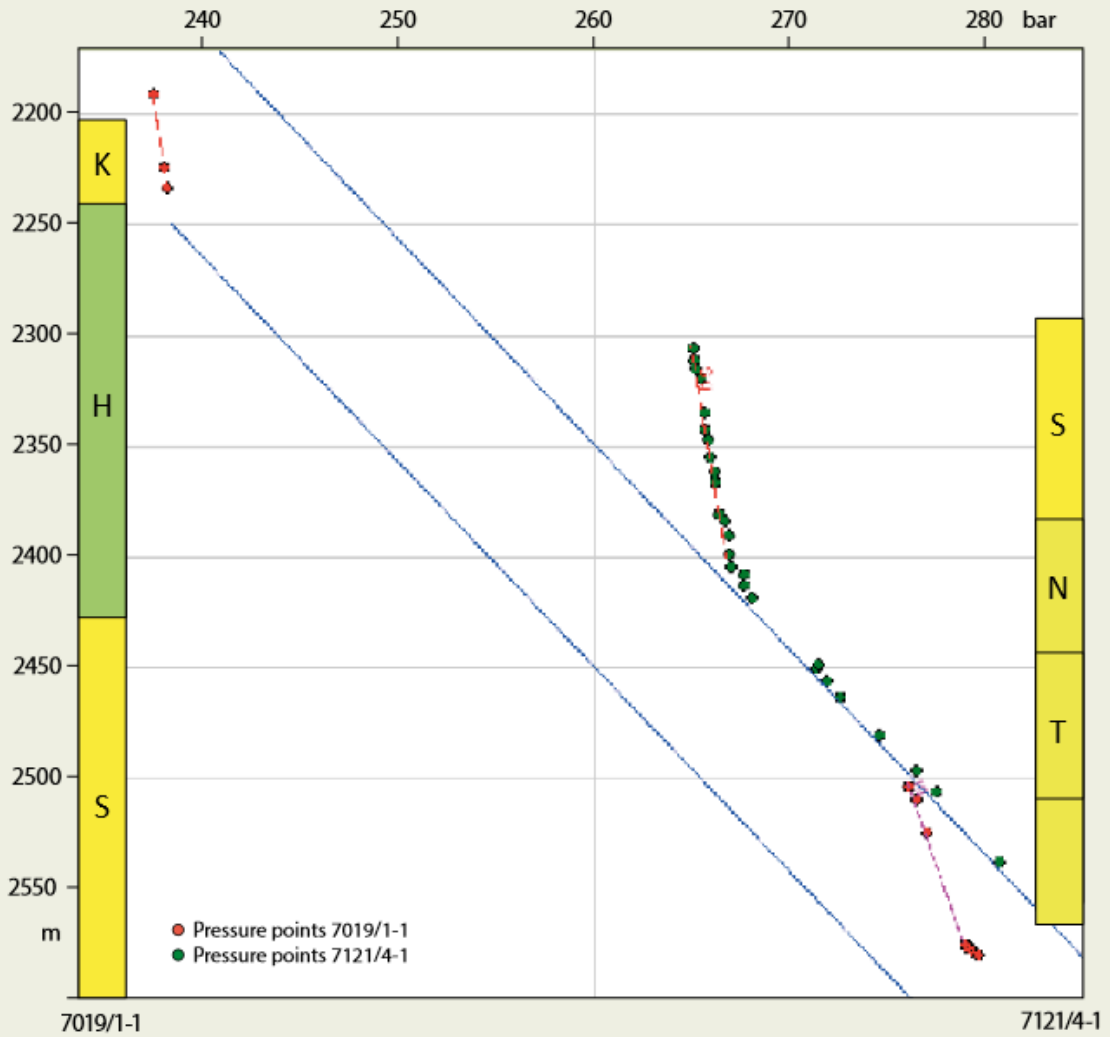

Fig. 3, Pressure vs. depth cross-plot showing the differences in pressure between the Lower Cretaceous and the Middle Jurassic reservoirs in well 7019/1-1 (left column, red dots) Halland et al. (2014)**.**

REGIONAL SETTING

Geologic setting of the Tromsø Basin

The study area is located inside the Troms-Finnmark Fault Complex (TFFC), in a segmented terrace which separates the Finnmark Platform to the southeast from the Tromsø Basin to the northwest (Fig. 4). Major structural elements relevant to the study area are; to the west the north-south elongated Tromsø and Harstad Basins, to the north the north-south elongated Ringvassøy-Loppa Fault Complex (RLFC), to the northeast by the Hammerfest Basin and to the east by the Finnmark Platform. The east-west striking fault system which separates the Hammerfest Basin by the Finnmark Platform is continuing across the study area, and separates the RLFC to the north by the TFFC to the south. The segmented terrace which makes up the study area is situated in an intersection between these major structural elements and fault complexes.

The southwestern Barents Sea has been influenced by several tectonic events, and the structural evolution of the area has been summarized by several authors (Breivik et al., 1998; Faleide et al., 2008; Faleide et al., 1993; Gabrielsen, 1984; Mosar et al., 2002; Riis et al., 1986; Rønnevik and Jacobsen, 1984; Øvrebø and Talleraas, 1977). The tectonic evolution of the area can be linked back to the Caledonian orogeny; in which long lived fault zones related to the Caledonian orogeny have influenced the tectonic development (Gabrielsen, 1984). Caledonian compressional deformation led to intracratonic weaknesses in basement rocks in the southwestern Barents Sea. Upper Devonian─Lower Carboniferous strike slip, led to the formation of northeast─southwest striking extensional grabens (Rønnevik and Jacobsen, 1984), in which large accumulations of Middle Devonian─Permian platform carbonates and large evaporates was preserved. Stable tectonic conditions caused progradation of Late Permian─Middle Jurassic clastics sourced from the east (Rønnevik and Jacobsen, 1984), which formed some of the most prolific reservoirs in the area (e.g., Late Triassic Tubåen Formation, Middle Jurassic Stø Formation). Middle Jurassic─Early Cretaceous rifting led to formation of deep north-south elongated basins in the western parts of the Barents Sea, which is a key event for this study.

Fig. 5 shows a plate model A─D the evolution from Late Jurassic to present. Plate (A), Fig. 5 shows the configuration during Kimmeridgian, a time when most of the Arctic Basins are connected and in relation to each other (Riis et al., 1986). During this time large amounts of organic rich source rock are deposited in the Barents Sea. This source rock is equivalent to Kimmeridge clay, and the formal name for the formation in the Norwegian

Barents Sea is the Hekkingen Formation. Towards Valanginian (Plate (B), Fig. 5) the clockwise rotation of Greenland, leads to the formation of north-south trending Cretaceous structural elements. Continued movement after the Jurassic rifting caused subsidence along major boundary faults with deposition of gravity flows into the basin from uplifted and eroded basin margins, in the Hammerfest, Tromsø and Bjørnøya basins(Seldal, 2005) Uplift of platforms and basement highs develop localized clastic wedges (Knurr Formation) in the southwest and shelfal progradation from the east. Late Cretaceous (Plate (C), Fig. 5) rifting related to the initial opening of the North Atlantic; reactivates parts of the Kimmeridgian rift systems in the west, and the major extension jumps across the Senja Ridge and forms the development of the Sørvestnaget Basin. Continuous development of the North Atlantic towards today (Plate (D), Fig. 5) caused Greenland to drift along the western margin of the Barents Sea and forming strike slip transpression and transtension along the Senja Fracture zone. Large accumulations of Cenozoic sediments are deposited towards the Sørvestnaget Basin and the Continent Oceanic Boundary (COB), which is related to the uplift and glacial exhumation of the Barents Sea.

The Senja Ridge today, has a high positive gravity anomaly (Fig. 4). The positive anomaly could imply that it consists of high density sedimentary rocks formed by the compression related to the strike slip movement (Riis et al., 1986; Øvrebø and Talleraas, 1977). The opposite gravity low of the Tromsø Basin is related to the deep Cretaceous and Cenozoic sedimentary succession in the basin.

Stratigraphy

A lithostratigraphic column summarizing the main tectonic events are correlated with well 7019/1-1 can be found in Fig. 6. Relevant surfaces for the study area and interval of interest are from Middle Jurassic to Lower Cretaceous.

Stø Formation

The Stø Formation is generally very dominated by well sorted mature sandstones. The formation is generally thickening towards west, and is thinning eastwards in the Barents Sea. The age has been defined between late Pliensbachian to Bajocian, with a diachronous base, younging towards east. The sandstones are deposited in a prograding coastal marine

environment, and the formation is one of the most prolific reservoirs in the Barents Sea (Dalland et al., 1988b).

Hekkingen Formation

The Hekkingen Formation consists of dark shales and claystones, with interbeds of limestone, dolomite, siltstone and sandstones. The clastics of the Hekkingen Formation are most common towards basin margins. The depositional environments change from marine, to deep marine with anoxic conditions. Minor sandstone intervals may exist internally in the Hekkingen Formation. The age of the Hekkingen Formation is from early Kimmeridgian to early Berriasian. The Hekkingen Formation is the most important source rock in the Barents Sea; its base is marked by a high gamma ray reading, usually situated at the top of the Fuglen Formation (Dalland et al., 1988b).

Knurr Formation

The Knurr Formation is generally defined as calcareous marine shale, consisting of dark to brown claystones, with limestone and dolomite interbeds (Dalland et al., 1988a). The formation is deposited in open and generally distal marine environments (Smelror et al., 1998). Sandstones in the Knurr Formation are best developed along the basin margins of the Hammerfest Basin, and are pinching out laterally towards the center of the basin. The formation is generally aged from late Berriasian to Barremian. It is time equivalent to the Klippfisk Formation (Smelror et al., 1998) (Barents Sea) and the Rurikfjellet Formation (Svalbard) (Grundvåg et al., 2013). Internal sandstones in the Knurr Formation seem to be slightly diachronous across the southwestern Barents Sea, which is related to the timing of events and uplift of different sediment sources.

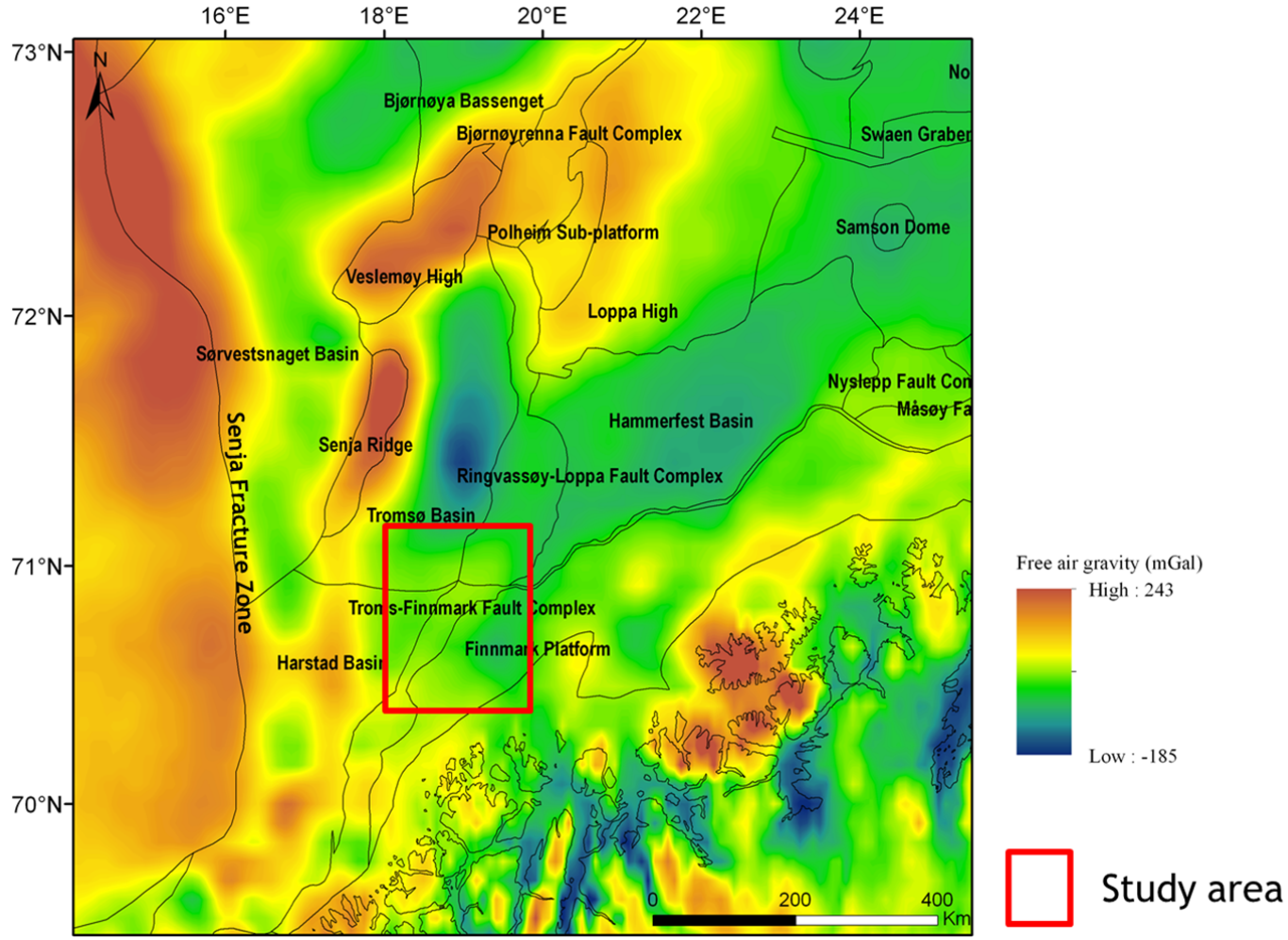

Fig. 4, Combined Gravity map and main structural elements in the study area.

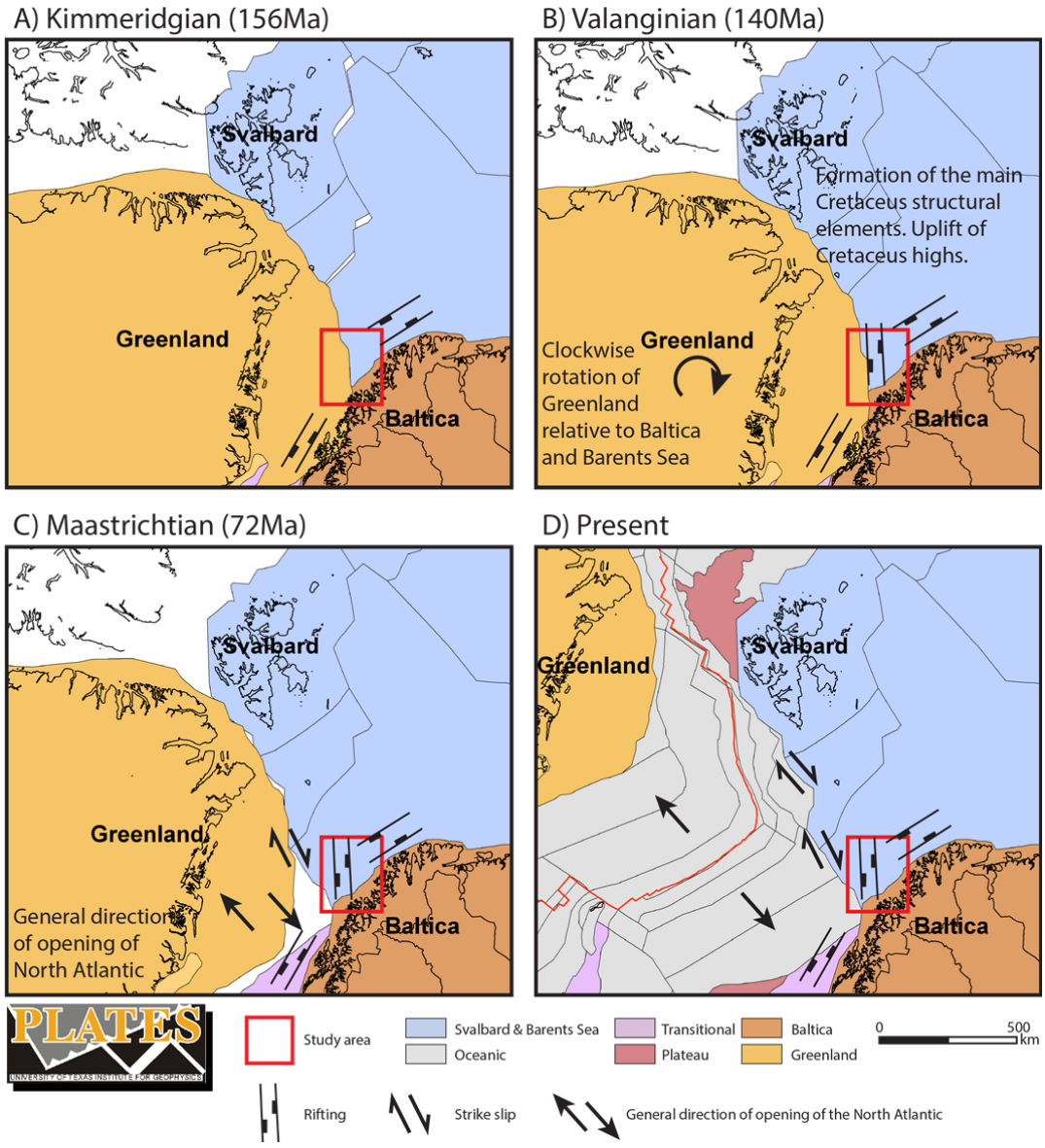

Fig. 5, Summarized plate model, illustrating the plate movements from Late Jurassic to present. From A-B Greenland is rotating, genereating the Early Cretaceous rift structures.C), the initial opening of the North Atlantic. D) Present day plate geometry of the North Atlantic and Barents Sea. The plate model is constructed in PaleoGis from the plate model provided by the Plates team at the University of Texas Institute for Geophysics.

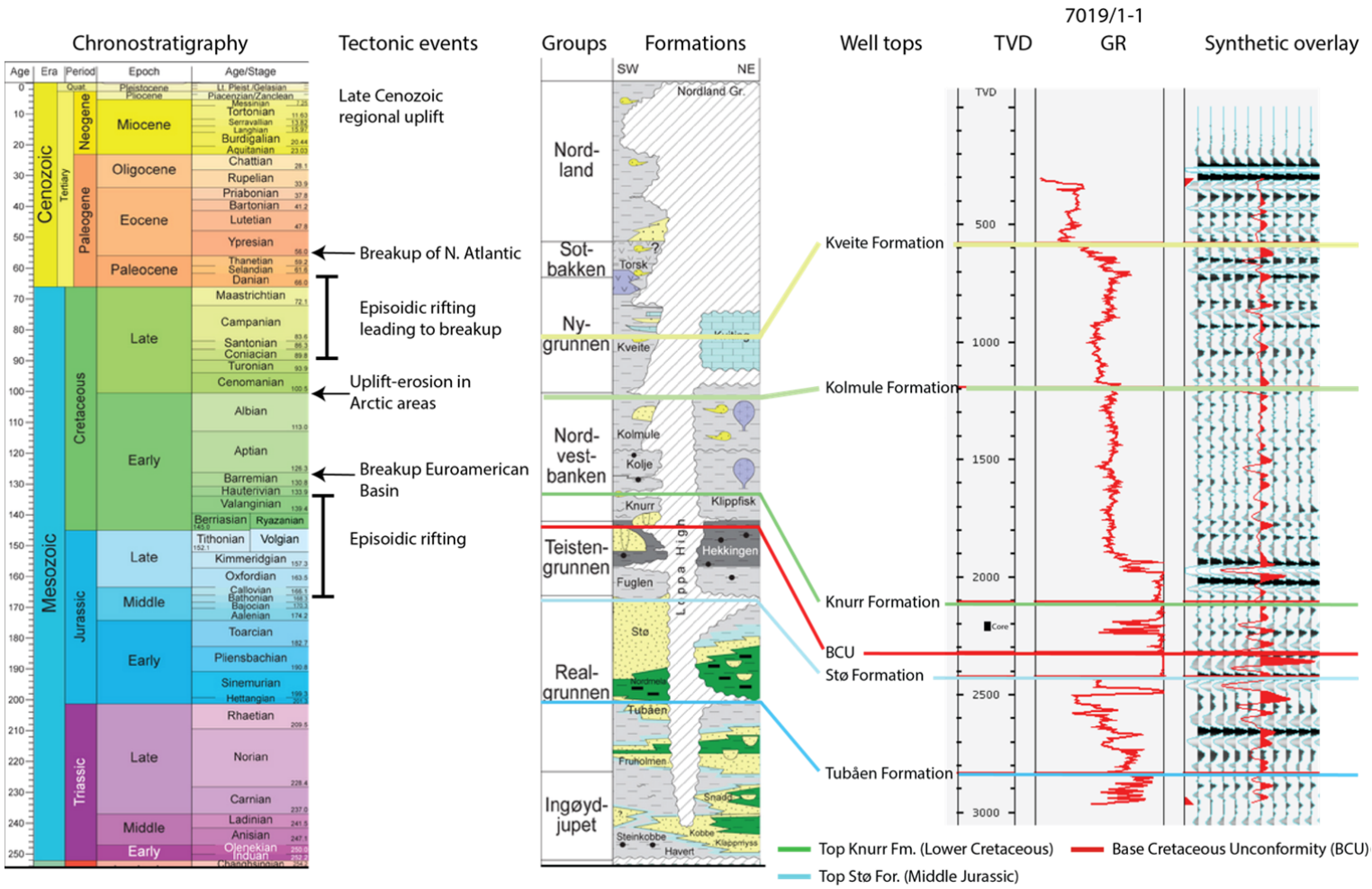

Fig. 6, Litostratrigraphic column correlated with synthetic and gamma ray of well 7019/1-1, and a summary of the main tectonic events for late Mesozoic and Cenozoic. Composed from (Gradstein et al., 2010; Smelror et al., 2009)

Observations from regional lines

Regional seismic line

Fig. 7) is starting from the east on the Finnmark Platform crossing the east-west fault system separating the platform from the Hammerfest Basin. The line continues into the Hammerfest Basin which has a large accumulation of Triassic and Jurassic sediments and crossing into the RLFC, which separates the Hammerfest Basin with the Tromsø Basin. To the west is the positive structural element the Senja Ridge which forms the western boundary of the deep Cretaceous Tromsø Basin. The RLFC structuring is related to the Middle Jurassic-Early Cretaceous rifting, which has a north south trend. The Base Cretaceous Unconformity drops deep into the Tromsø Basin west of RLFC, and is no longer visible towards the basin. The basin is bounding towards the uplifted Senja Ridge in the west.

Regional seismic line (Fig. 8) is striking from southeast to northwest and crossing the study area away from the Finnmark Platform. Observation from the line is to the southeast a tilted Permian platform below the Mesozoic interval. The late Jurassic to early Cretaceous rift structuring (red box, Fig. 8) in the TFFC is interpreted concave listric normal faults with the concave part facing the Finnmark Platform. These faults are being offset by a larger fault system of late Cretaceous which forms the deep Cretaceous Tromsø Basin in the west similar as in (Fig. 7). The deep Cretaceous succession in the Tromsø Basin is undifferentiable with an abundance of low amplitude reflections. Several chaotic reflections and with higher amplitudes indicates probable shale tectonics in the basin. A large anomaly in the acoustic impedance is observed deep in the basin. This is probably the southern elongation of the Senja Ridge. The Cenozoic succession is thickening towards west and prograding towards the continent oceanic boundary.

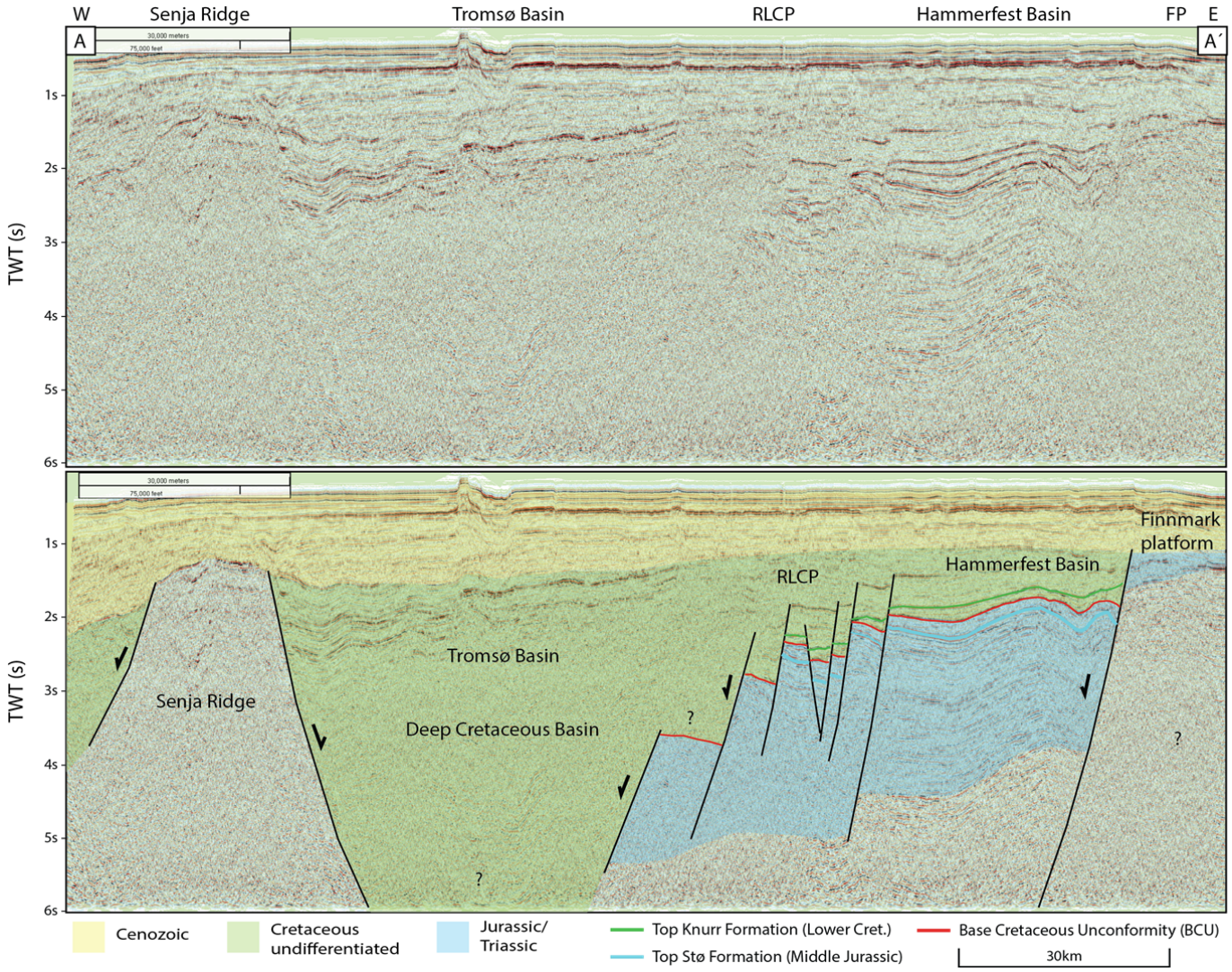

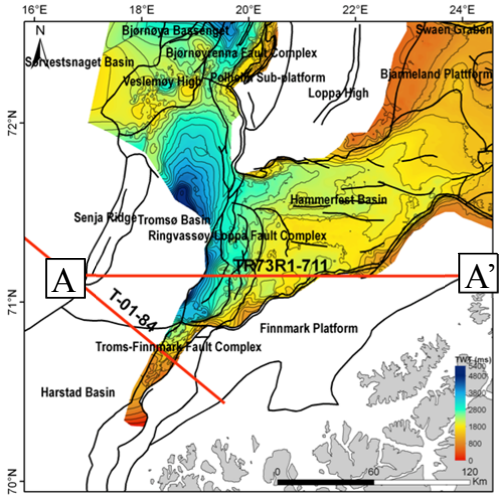

Fig. 7, Interpreted and uninterpreted regional seismic line TR-73R1-711. A'—A crossing the Finnmark Platoform into the Hammerfest Basin towards the Ringvassøy Loppa Fault Complex, into the Tromsø basin and towards the Senja Ridge to in the west.. Upper Right: Base Cretaceus Unconformity map with location of the line.

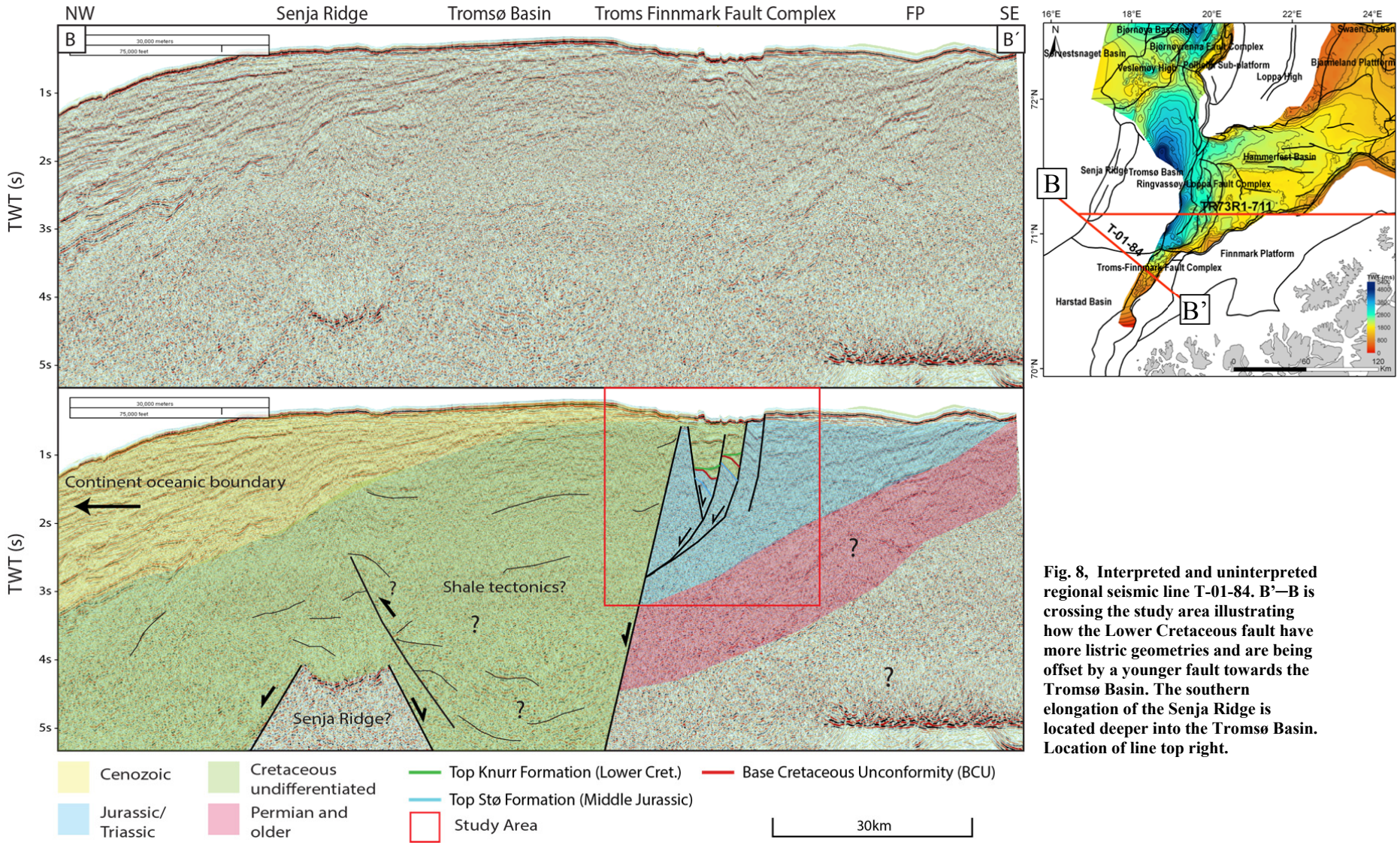

Fig. 8, Interpreted and uninterpreted regional seismic line T-01-84. B'—B is crossing the study area illustrating how the Lower Cretaceous fault have more listric geometries and are being offset by a younger fault towards the Tromsø Basin. The southern elongation of the Senja Ridge is located deeper into the Tromsø Basin. Location of line top right.

Theoretical background on rift basins

Fault displacement play an important role in the internal drainage development in extensional basins (Copestake et al., 2003). Drainage systems in extensional basins contain information about fault zone structures and the development of each individual fault segment. (Leeder and Jackson, 1993; Ravnas and Steel, 1998).

The evolution of normal faults can be subdivided into three main stages (Gawthorpe and Leeder, 2000):

Initiation (Fig. 9, 10, (A)):

In the normal fault initiation stage, large amounts of minor ruptures and fractures will start to form and generate smaller individual depocenters. The fault displacement is shared by several smaller faults, and the individual offset of each fault is minor.

Interaction and linkage (Fig. 9, 10, (B)):

Fault segments will start to become more developed, and minor ruptures will die out (e.g., faults Y and Z (Fig. 10 (B)). The tip of the faults will start to drift away from the center of the fault. Faults will start to interact, in which the tips are overlapping and generate a soft link between each other, generating relay zones in between them. Eventually larger faults will link up, generating hard linked zones consequently breaching relay ramps (Fig. 9 (B)).

Through going fault zones (Fig. 9, 10, (C)):

The fault segments are linking up causing larger individual fault displacements and lengths.

Footwall uplift and impact on paleodrainage: As faults propagate, the subsequent footwall uplift will start to affect the antecedent drainage systems (Fig. 11). In particular will fluvial currents follow the basin morphology, tend to shift directions and go around the tip of faults, into fault relay zones where there is less uplift. Continuous rotation of the fault blocks can shift the direction of antecedent fluvial systems completely, and cause the drainage to follow in an axial direction along the strike. A fluvial system may be able to maintain its antecedent direction, only if it is able to cut through the uplifting footwall, which causes the sediments to be fed into the hangingwall in an orthogonal direction away from the fault. More localized sedimentation with smaller catchments which have an orthogonal direction adjacent to the faults, are sourced from the incipient footwall catchment, and fault scarp degradation.

Marine rift basins may represent a large range of depositional processes (fig. 12) (Ravnas and Steel, 1998). These types of rift basins have variable syn-rift sedimentary architecture, and the controls on the internal architectures are changes in relative sea level, accommodation space, and sediment flux. The depositional processes making up the internal architecture of the rift basin, will have distinctive characteristics in the seismic expressions (Jackson et al., 2008); Prosser (1993).

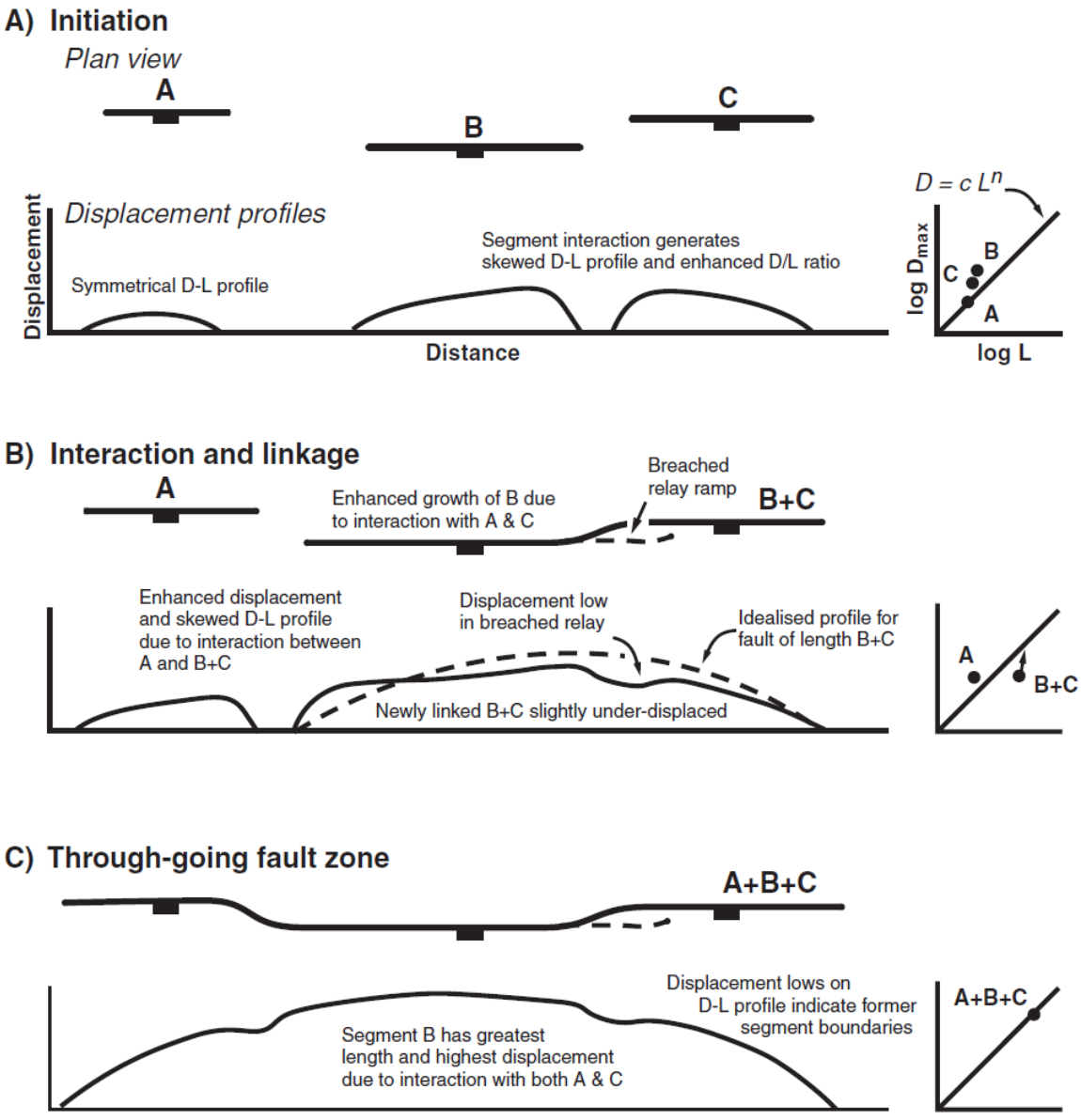

Fig. 9, Schematic evolution of three segments, following the three stages of fault evolution, with displacements profiles. Notice how the displacement profile in stage C) is similar to the displacement profile of fault A in stage A). (Gawthorpe and Leeder, 2000)

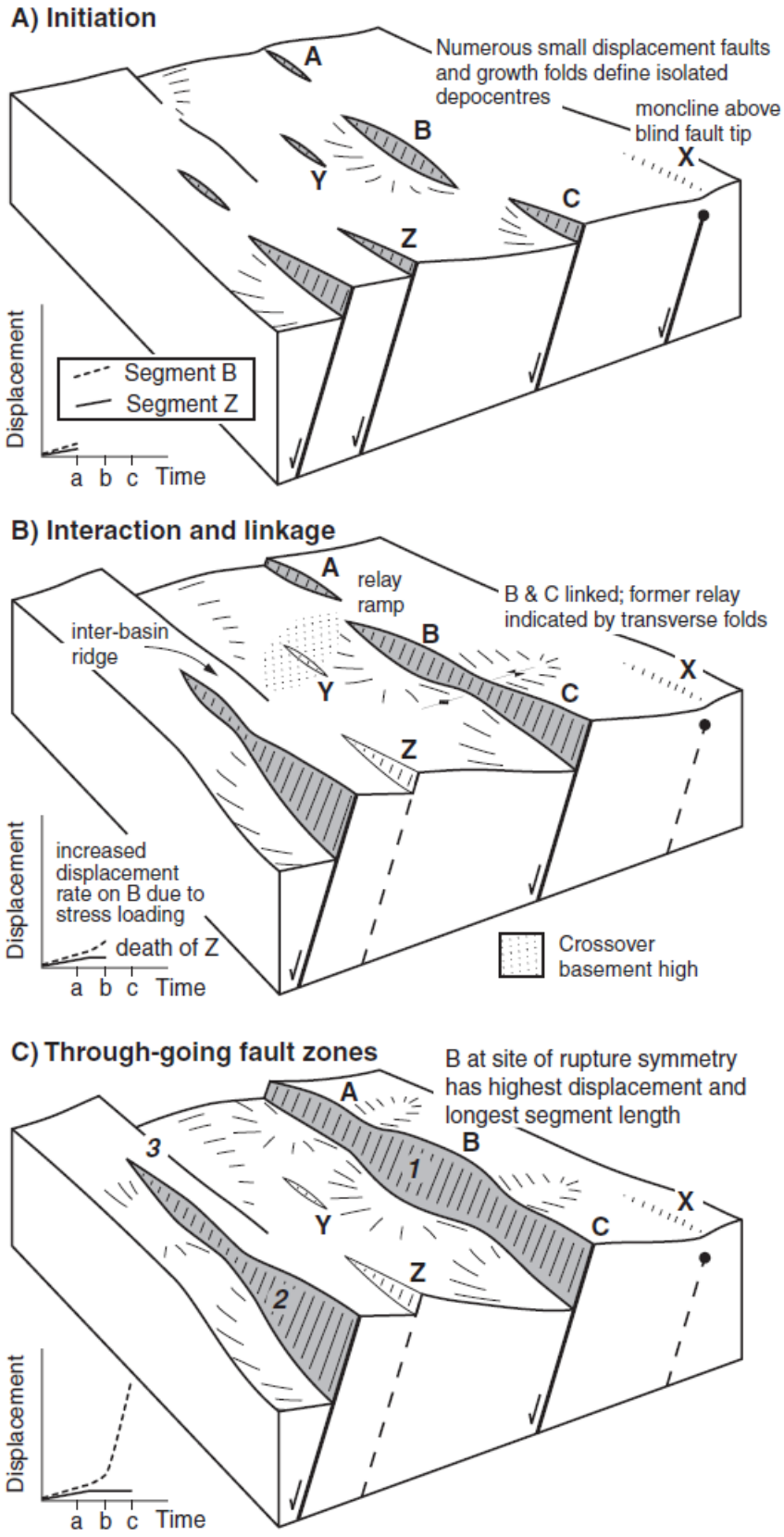

Fig. 10: Block diagrams illustrating the evolution of the three stages. Notice how faults like Y and Z forms during the initiation stage, but later become inactive. (Gawthorpe and Leeder, 2000)

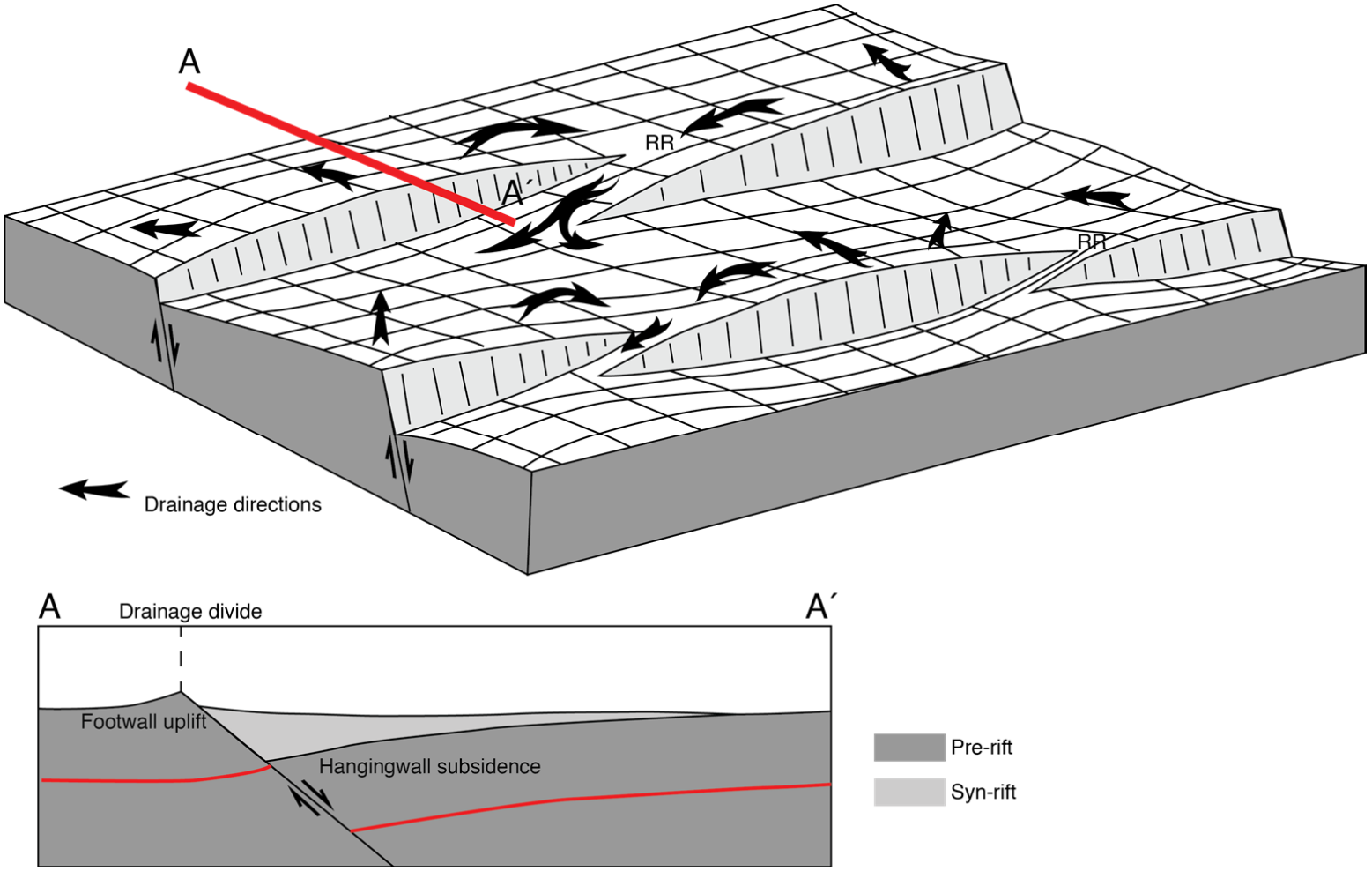

Fig. 11, Block diagram with grid indication how the internal relief of half grabens will control the sediment dispersal. A-A' shows a cross section through a half graben, indication how the flexural footwall uplift will form a drainage divide in which sediment dispersal shifts away from the fault. Syn-rift sediments are forming a syn-tectonic wedge towards the adjacent fault. RR: Relay ramp. Modified from Ravnas and Steel (1998)

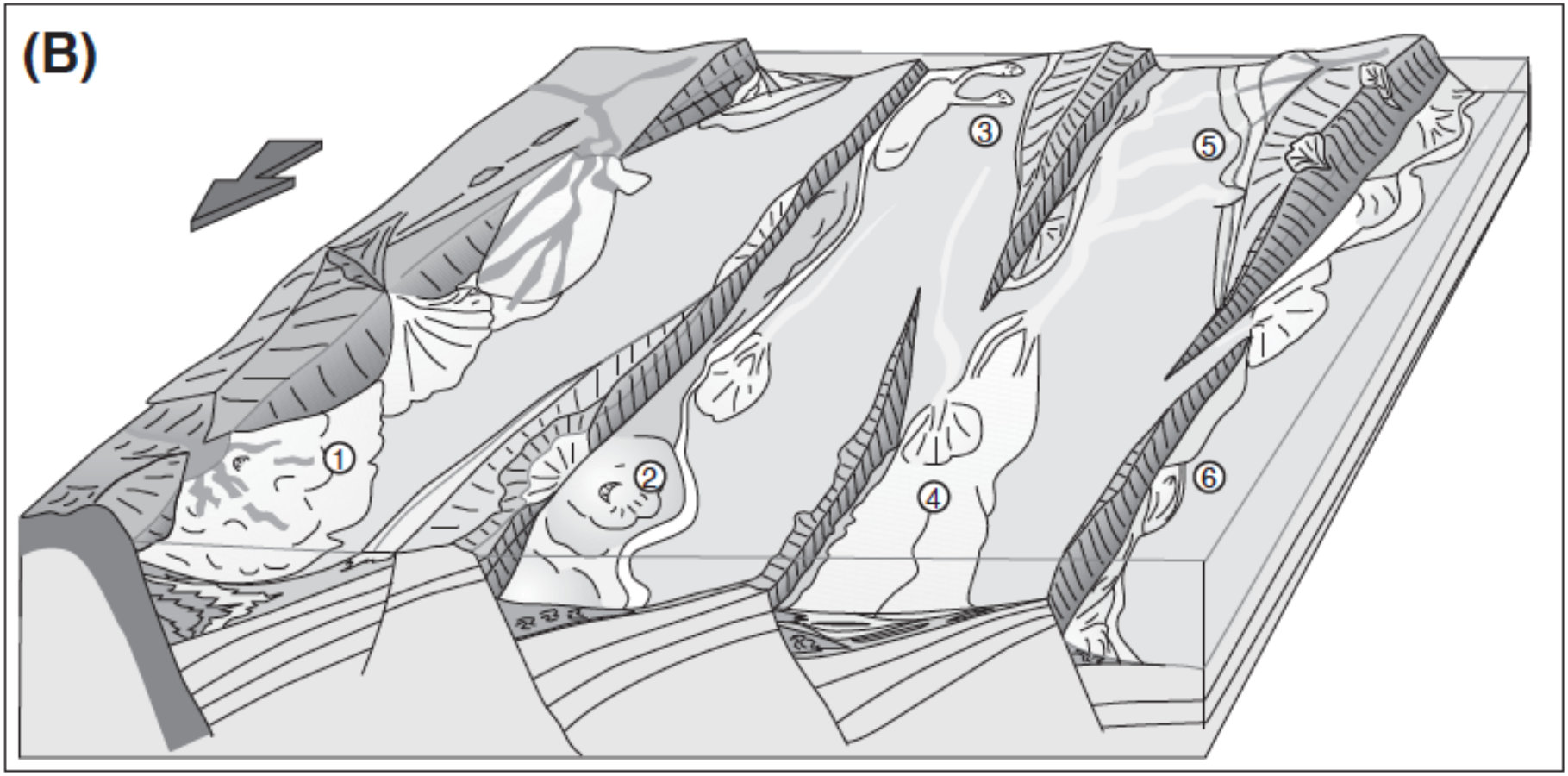

Fig. 12, idealized illustration of depositional environments of marine to deep-marine rift basins (left to right). Several processes of drainage are involved, orthogonal deposition sourced from adjacent faults and axial deposition into relay zones and along the faults. (Ravnas and Steel, 1998)

DATABASE AND METHODS

Seismic Data and Well Data

This study uses extensive 2-D seismic surveys and one 3-D seismic data set NA-94-3D, along with core, well logs, geochemical and final well reports of well 7019/1-1 (Fig. 13). The 3-D data was gathered by Norsk Agip AS in 1994 and has a total length of 48191km (NPD). The survey is post stack conventional 3-D data with 12.5m x 15m line spacing. A complete list of the surveys used in this study is listed in (Appendix 1). All the provided data are collected from the Diskos PetroBank, along with official well tops from the Norwegian Petroleum Directorate (NPD). IKU shallow core well 7018/5-U-1 has been included in the database map, as it contains a time equivalent cored interval of the Lower Cretaceous on the Finnmark Platform. The interval has been described by Smelror et al. (1998); Smelror et al. (2001), which has provided useful understanding of the regional setting during Lower Cretaceous.

Data quality

The quality of the seismic surveys is ranging from good to poor. Sea bottom multiples are a common issue in the Barents Sea, and are affecting parts of the interval of interest. Amplitude vs. frequency cross plot (fig. 14) illustrates the differences in the frequency bandwidth of three surveys used in this study. The dominant frequency of the 3D data is centered round 10Hz, which is low compared to the 2D surveys (25Hz). The frequency has a large impact on the vertical resolution, as a lot of the beds are below the tuning thickness of the seismic (Fig. 15). According to Chopra et al. (2006) an average frequency centered around 30 Hz will not have base and top reservoir resolved with thicknesses less than 25m (i.e. tuning thickness). Consequently we may expect seismic tuning thickness of the 3D seismic data more than 60m and 30m for the 2D.

Study Methods

Landmark DecisionSpace® software from Landmark Graphic Corporation (LGC) was used for the seismic and well interpretation. Synthetic well tie was calculated from the well 7019/1-1 with Landmark's SynTool® and tied with the 3-D dataset (Fig. 6). Intepretation of the 3D horizons was carried out with an by every 50th line along the strike of the structure and down to every 10th line in the dipdirections. The 2D interpretation was generally focused in the southern parts of the study area outside the coverage of the 3D. The maps were generated in DecisionSpace® by gridding the interpreted horizons, either by 50x50m or 100x100m refinement gridding, and finalizing of maps was done in ArcMap 10.1. Seismic attribute maps were extracted from the Top Knurr Formation surface. Seismic facies maps were made from observations of seismic character reflectivity, continuity and lateral variabilities of the Lower Cretaceous syn-rift interval. The facies maps are constructed from the 2D data, which were mapped out with polygons. The cored Lower Cretaceous interval of well 7019/1-1 was logged at the Norwegian Petroleum directorate (NPD) main offices in Stavanger.

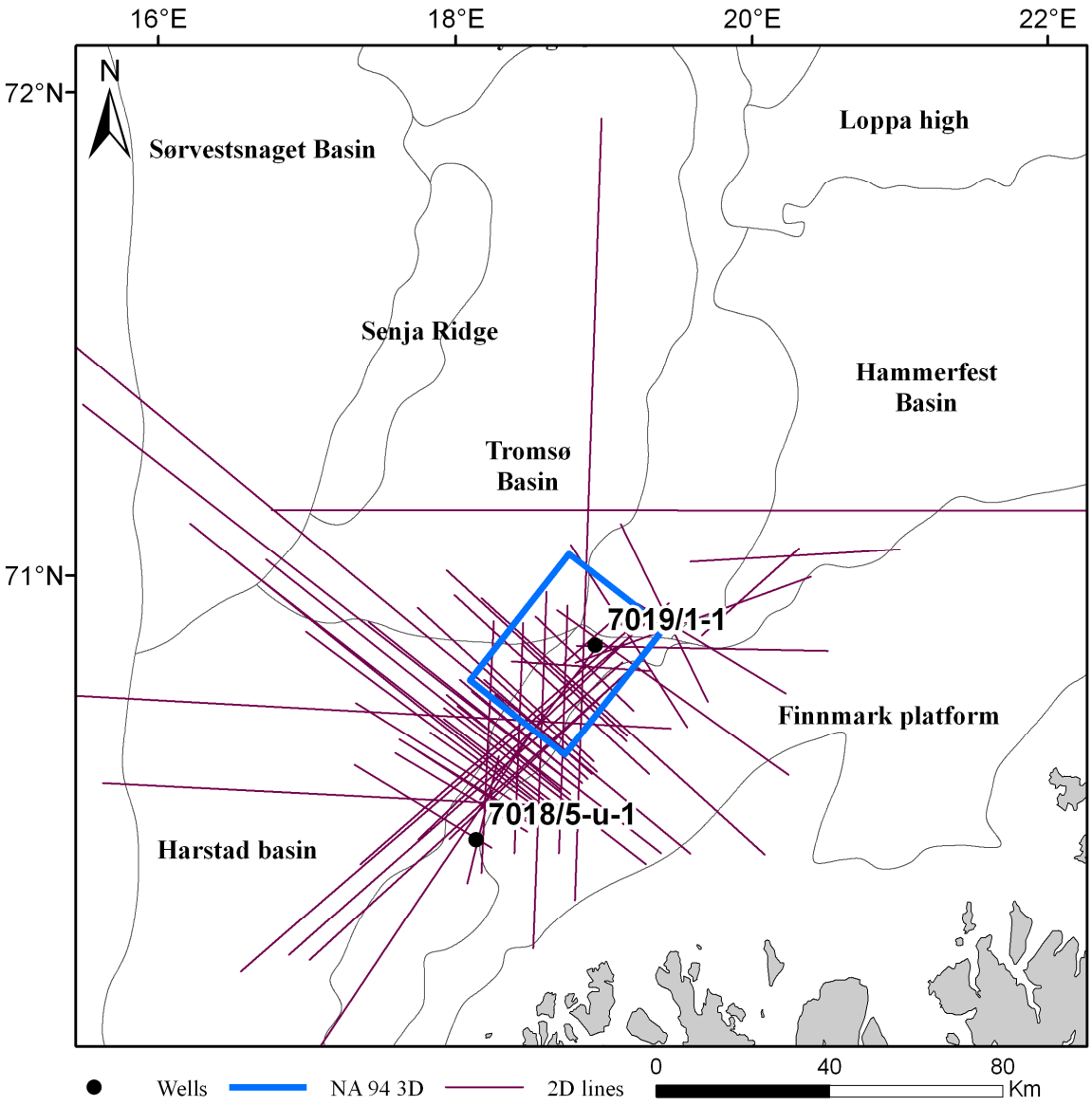

Fig. 13, Seismic and well database map.

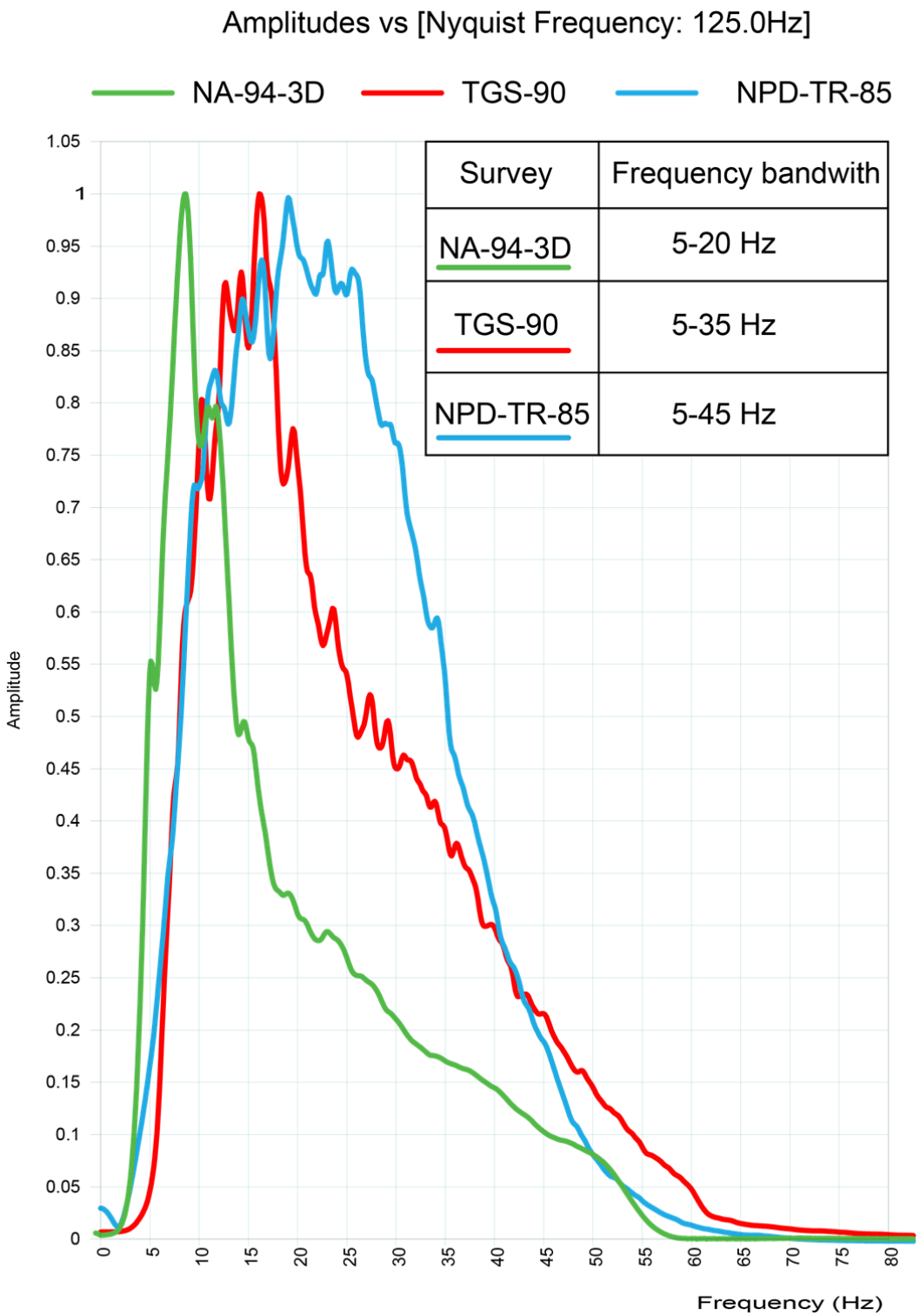

Fig. 14, Amplitude vs. Frequency plot of three surveys in the dataset used in this study. Especially the low frequency bandwidth of the 3D survey (green line) indicates that the 3D has low vertical resolution

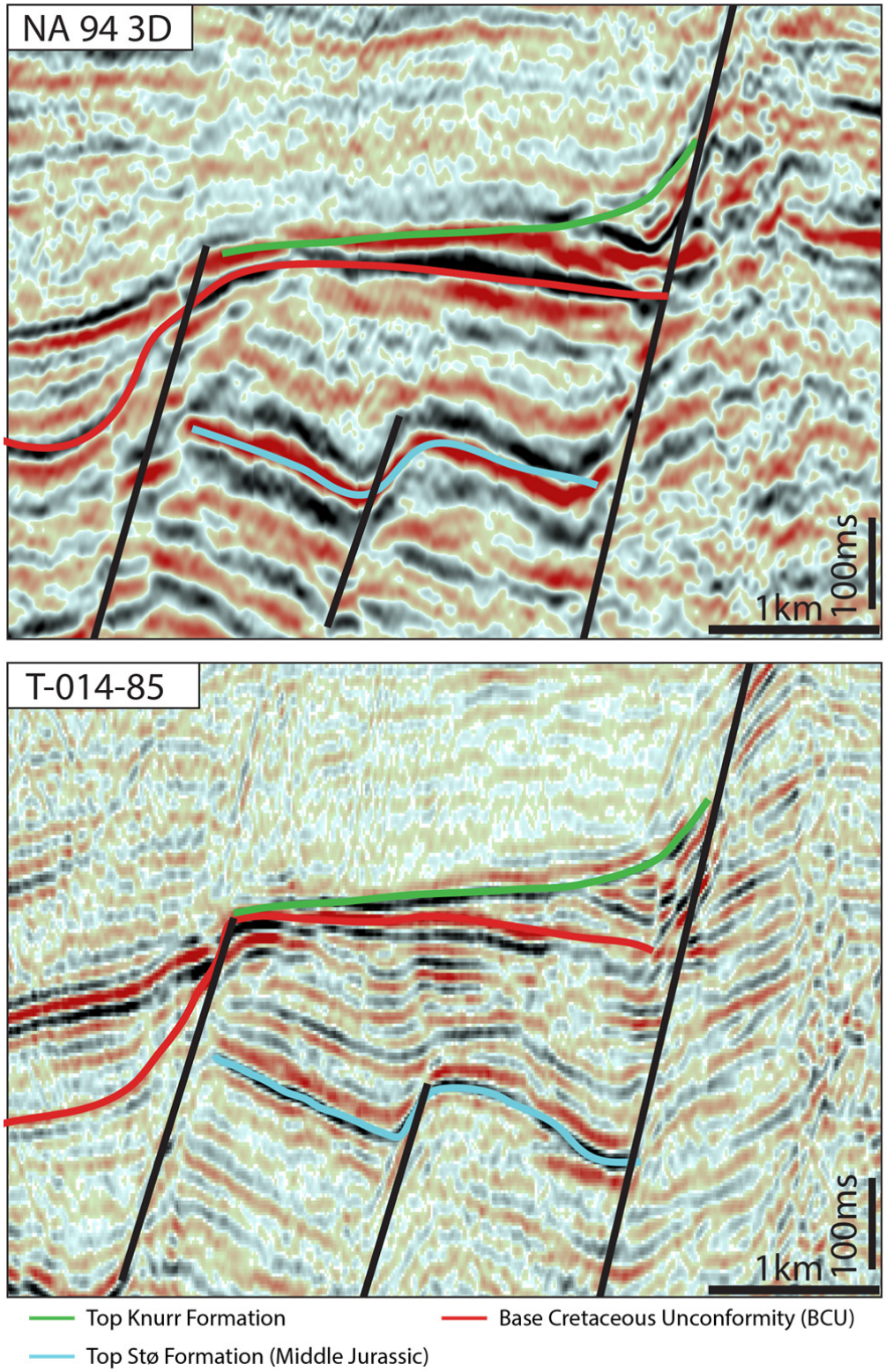

Fig. 15, Comparison of the vertical resolution of the seismic surveys. Illustrating the low frequency of the 3D compared to the 2D data. The 3D line has a random direction to mimic the navigation of T-014-85 (from NPD-TR-85 Fig. 16).

OBSERVATIONS

Well and core description of well 7019/1-1

14m's of core was collected from the Knurr Formation in well 7019/1-1. Following is a description of the observations from the logs and identified lithofacies from the available core. Figure 16, shows the lithological log column from the cored interval, correlated with the logs from the well. The well logs are focused on the main reservoirs penetrated in the well with focus on the Knurr Formation. A table of the lithofacies along with example pictures are listed in table 1. Complete images of the core along with the lithologic log with descriptions can be found in appendix 2 and 3.

Well log characters

Knurr Formation (Lower Cretaceous)

The gamma ray and density-neutron logs are indicating that the Knurr Formation generally seems to be dominated with shale towards the top and base forming possible seals in each direction. Four separate sandstone reservoirs can be observed with a net sand of 52m (Seldal, 2005), each of the reservoirs zones has a corresponding increase in the ressistivity indicating hydrocarbons.

Hekkingen Formation and Fuglen Formation (Upper Jurassic)

32m of the Hekkingen Formation are present in the well, which is quite low for the formation (359m in the type well and 113m in the reference well, (Dalland et al., 1988a)), and it is probable that there have been signinficant erosion of it at the well location. At the base of Hekkingen Formation there is an increase in the gamma-ray prior to entering the Fuglen Formation. The shales of Hekkingen and Fuglen Formation probably forms a good seal between the Stø and the Knurr Formation.

Stø Formation (Middle Jurassic)

Low gamma ray readings are indicating good clean sandstone reservoirs in the Stø Formation, seperated by shales. The high ressistivity readings correspond to the precense of hydrocarbons. The water contact in the Stø Formation contact is not showing in (Fig 16), but can be seen in the pressure plot in (Fig. 3).

Lithofacies

Lithofacies 1 (LF1) consists of heterolithic mudstones mixed with thin (1-4mm) stringers of siltstone. The interpretation of LF1, is that the mudstones represents a mix of hemipelagic mud interbedded with distal stringer of turbiditic currents. The hemipelagic mudstones represent basinal background sedimentation interfingered with low density turbiditic currents representing far distances of travel (Table 1, Fig.16, LF1).

Lithofacies 2 (LF2) consist of poorly sorted mixed mudstone and silstone with larger clasts (0.5-2cm) of silstone, mudstone and sandstone. LFC is matrix supported with the dominant matrix of mudstone. The interpretation is that these deposits are related to localized muddy debris flows which represent shorter distance of travel (Table 1, Fig. 16, LF2).

Lithofacies 3 (LF3) consists of massive medium grained sandstone, with a sharp base. There is minor to none changes in the grainsize, and the sandstones are more or less structureless. The interpretation of these sandstones is that they represent high density turbidites. The beds does not seem to be amalgamated, and it seems like each bed represent one single turbiditic lobe (Table 1, Fig. 16, LF3). The sandstones of LF3 corresponds to the low gamma ray readings in the Knurr Formation (Fig. 16).

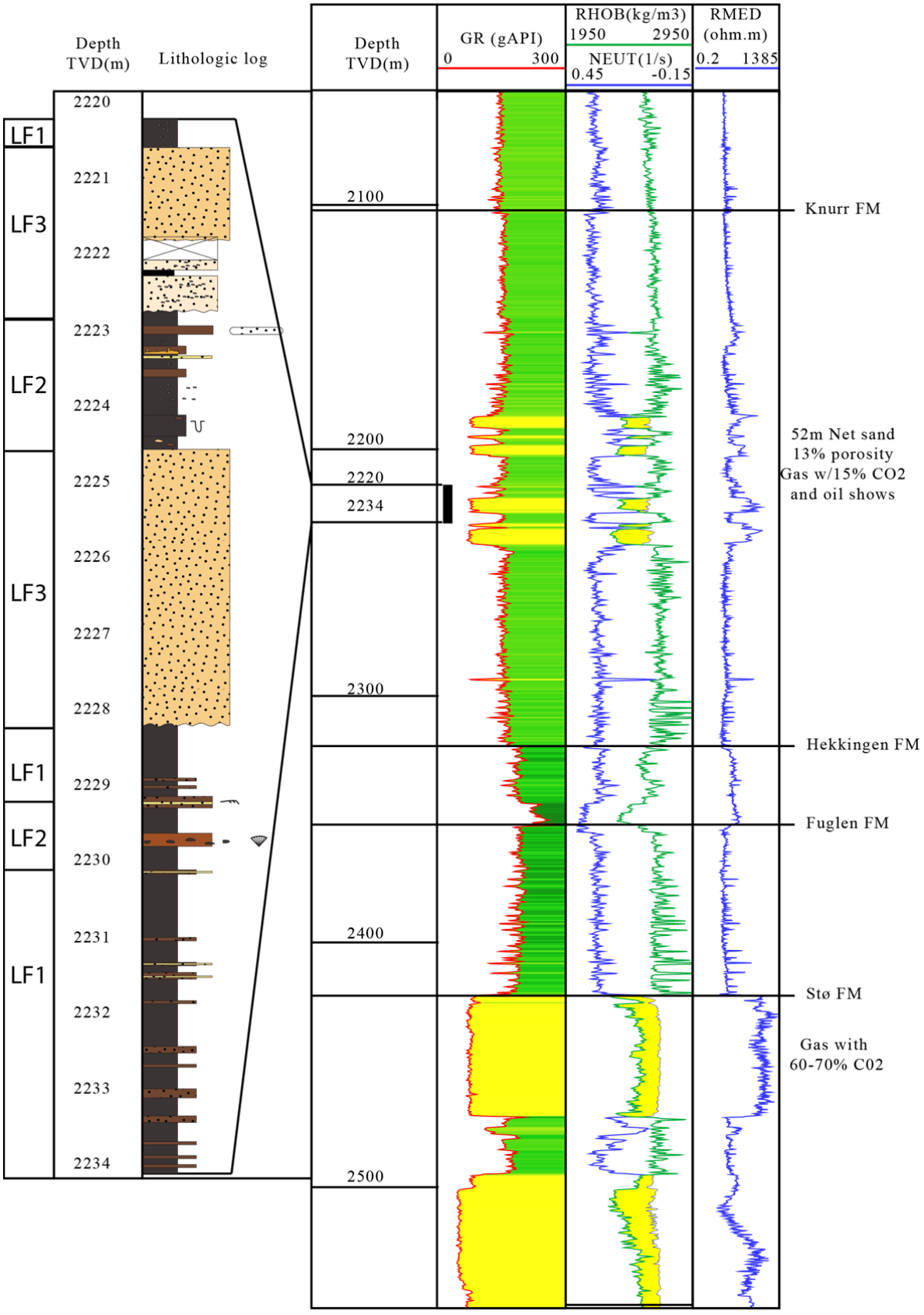
Depth TVD(m)
Lithologic log
LF1
LF3
LF2
LF3
LF1
LF2
LF1
2220
2221
2222
2223
2224
2225
2226
2227
2228
2229
2230
2231
2232
2233
2234
Depth TVD(m)
2100
2200
2220
2234
2300
2400
2500
GR (gAPI)
0
300
RHOB(kg/m3)
1950
2950
NEUT(1/s)
0.45
-0.15
RMED (ohm.m)
0.2
1385
Knurr FM
52m Net sand
13% porosity
Gas w/15% CO2
and oil shows
Hekkingen FM
Fuglen FM
Stø FM
Gas with
60-70% C02

Fig. 16, Well 7019/1-1 lithological column of the core, correlated with gamma ray, density-neutron and ressistivity logs. Black bar indicate the interval of the core.

Table 1, description, interpretation and examples of the main lithofacies identified in the Knurr Formation in well 7019/1-1.

Litho-Facies	Description	Interpretation	Examples
LF1	Dark mudstone with stringers of 1-4mm siltstone.	Basinal deposits, hemipelagic mudstones mixed distal stringers of deep marine turbidites.	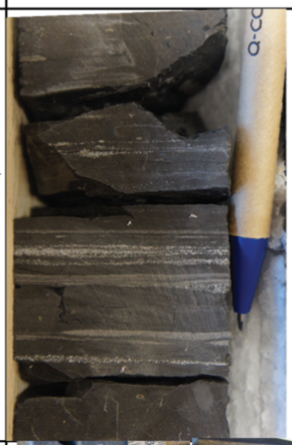
LF2	Unorganized, chaotic, mudstone with clasts of mudstone, silstones, and siderites. Matrix supported and structureless	Localized debris flows.	
LF3	Medium grained sandstone. Massive, well sorted.	High density turbidites	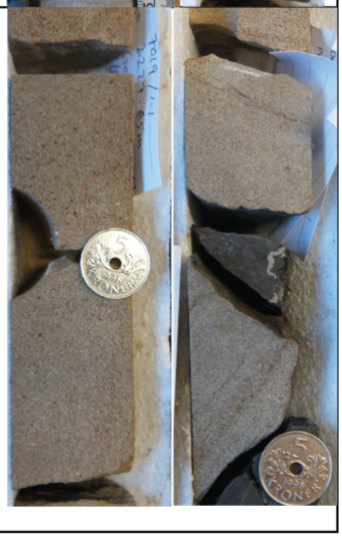

Structural interpretation

Main surfaces used for the structural interpretation are the pre-rift top of the Stø Formation, BCU and top of the syn-rift Knurr Formation. Three main fault families (FF1, FF2, and FF3) have been identified in the study area. Maps and cross sections of surfaces and faults are shown in (Fig. 17, 18, 19, 20, 21, and 22).

Fault Family 1 (FF1) is striking WSW-ENE (Fig. 17, 18, 19), and separates the TFFC in the south with the RLFC in the north. The fault is an extension of the WSW-ENE fault system which separates the Hammerfest Basin from the Finnmark Platform (
Fig. 7). The FF1 seems to have been reactivated through several stages, which corresponds well to understanding of these fault systems described by (Gabrielsen, 1984). The detachment of these faults is probably related to deformation in basement and cannot be resolved in seismic. FF1is easy to trace along the margins of the Hammerfest Basin, but it gets more complex into the TFFC, due to interaction with FF2 and FF3. FF1 defines the northern limit of the structure, and separates it from the RLFC.

Fault Family 2 (FF2) (Fig. 17, 18, 19, 20) consists of a cluster of SW-NE striking normal faults. The faults are interpreted to be listric with the concave part facing the Finnmark Platform. The structure is bounded by a large fault of FF2 to the east which separates it by the Finnmark Platform (Fig. 19, 20, blue line). The faults are tipping in both directions along their strike, and are causing the structure to be heavily segmented. A more detailed description of FF2 follows in the observations of the surfaces and the evolution of FF2 is included in the discussion.

Fault Family 3 (FF3) (Fig. 17, 19, 20) shares the same SW-NE strike as FF2, and marks the eastern boundary of the Cretaceous Harstad and Tromsø basins. FF3 might have been part of FF2 but has been interpreted as a separate fault family due to the large offset it has in contrast to the smaller offset faults of FF2. Reactivation of FF3 seems most likely involved in basement deformation, with the largest offset towards Late Cretaceous, related to the formation of the deep Cretaceous basins in the west.

Structural configuration of surfaces

Stø Formation

The top of Stø Formation (Fig. 21) has been used to make a structural configuration of the pre-rift surface. Interpretation of the Stø Formation reveals several smaller displacement faults, which can be observed several places along the structure (line B-F (Fig. 19, 20)). There seems to be a higher abundance of these smaller faults in the northern parts of the structure seen in the map (Fig. 21) and line B (Fig. 19). Erosion of the Stø Formation can be seen in the southern parts of (Fig. 18), southeastern parts of lines A-C (Fig. 19) and western part of line E (Fig. 20). Faults with larger displacement of the Stø Formation seem to have similar offset as the BCU.

Base Cretaceous Unconformity (BCU)

The BCU surface is heavily segmented along the structure, but less than the Stø Formation. Larger offset faults off FF2 are forming several depocenters along the strike of BCU. The surface drops deep towards north, offset by FF1, and the continuation north of FF1 is unclear. The surface has not been interpreted towards west as it is offset by FF3 and is too deep to be resolved. On the Finnmark Platform the surface is eroded and is no longer present.

Knurr Formation

The top of the Knurr Formation, (Fig. 22), appears as a lot less faulted than the BCU and the top of Stø Formation. The surface distribution is controlled by the faults of FF2 draping on top of BCU.

Segmentation of FF2

The structure is divided into several segments by FF2, and gets narrower towards the south and is at its widest around diplines C-E (Fig. 19, 20). In the area where the structure is wider, it is more segmented, and more faults are involved. As several faults are involved in the offset along these segments, the total displacement across the structure is shared between them. In turn this result in smaller individual offset of the faults to the north and a larger individual offset of the faults in the south (line F (Fig. 20). The faults are tipping towards north and towards south, generating along strike depocenters with the largest depocenters in the south, due to less faults. Typical structural elements identified in the structure are relay ramps, breached relay ramps, narrow grabens, horsts and half-grabens (Fig. 17). Together these structures make up intrabasinal transfer zones for sediment dispersal, and separate depocenters which will trap sediments.

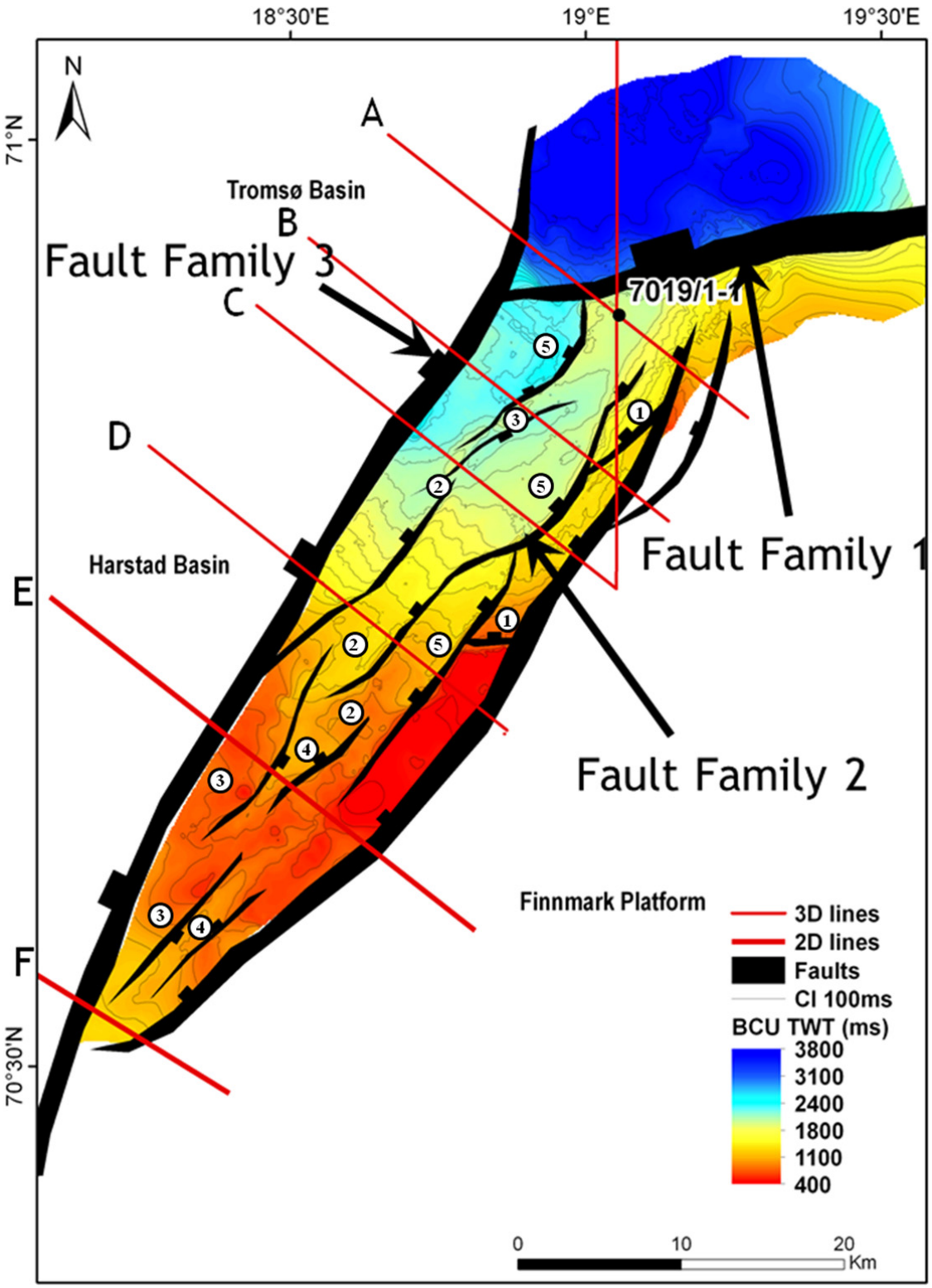

Fig. 17, Base Cretaceous Unconformity time structural map, with main faults families and locations of N-S tie line (Fig. 18), and diplines A-F (Fig. 19, 20). 1: Breached relay. 2: Relay ramp. 3: Horst. 4:Graben. 5: Half-graben.

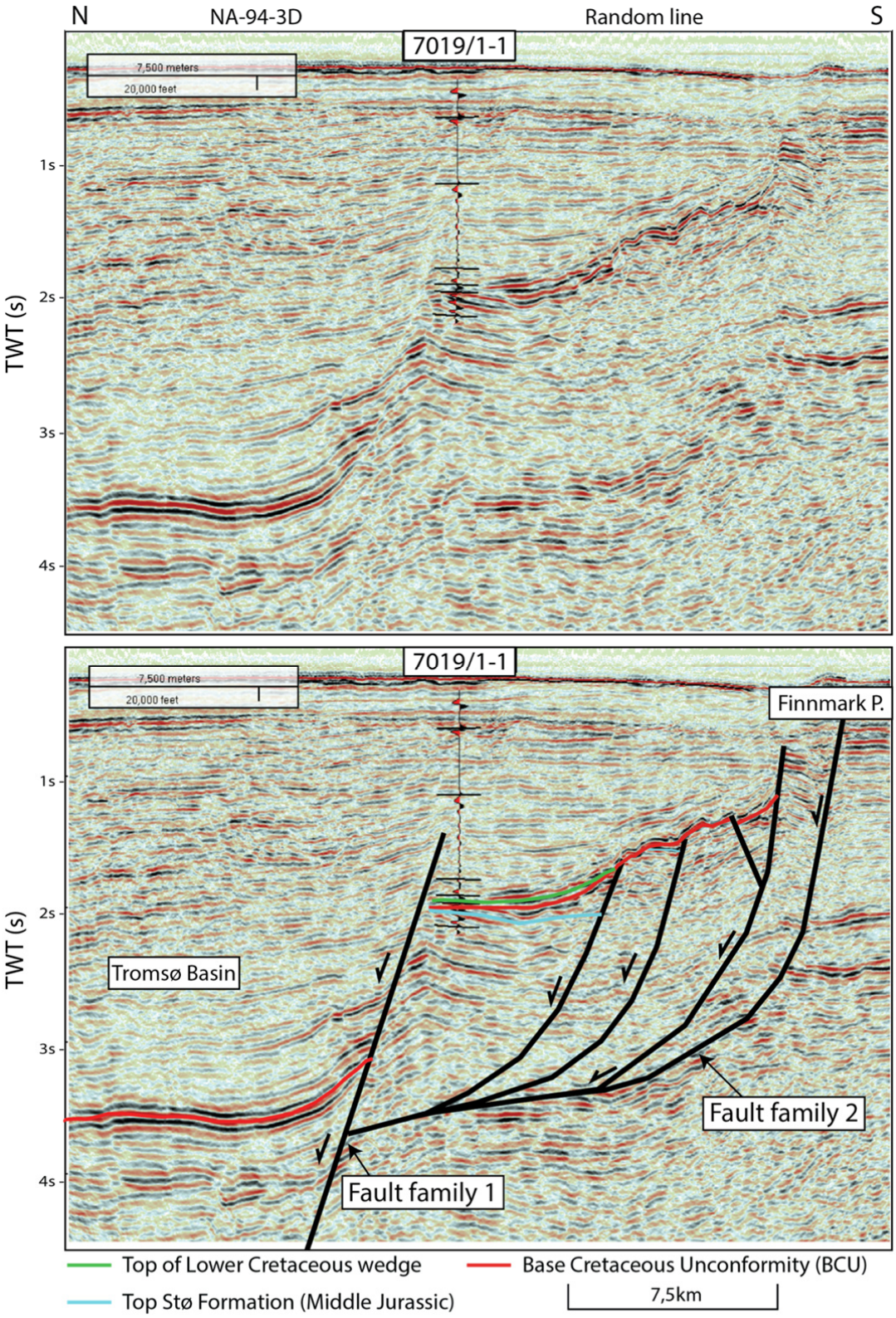

Fig. 18, N-S seismic random well tie line. Showing main horizons interpreted, and the structural deformation styles of the area crossing FF1 and FF2. Location of line is shown in figure 17.

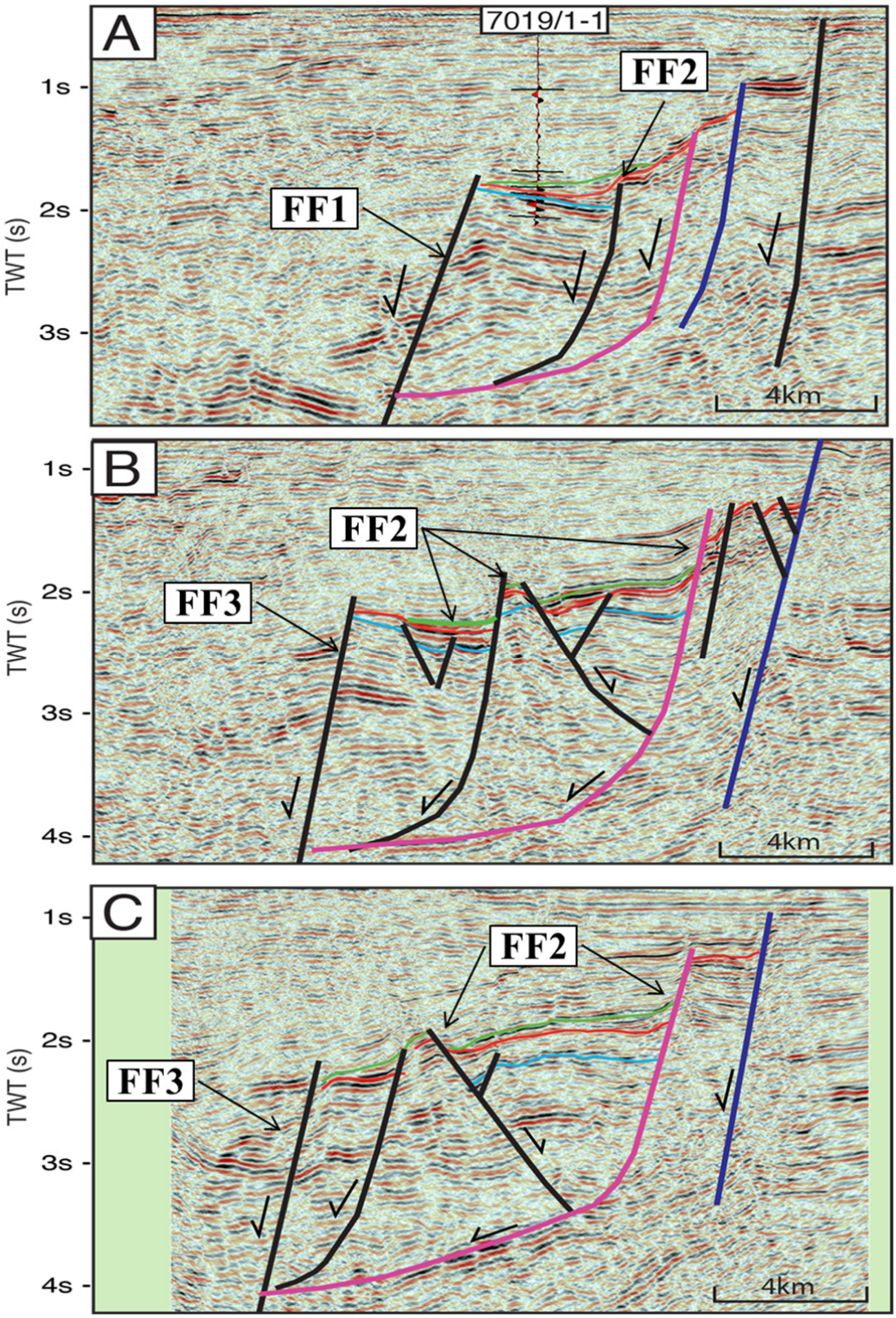

Fig. 19, Diplines A-C showing how the segmented structure is changing along strike. Blue line: Top of Stø Formation, Red line: BCU, Green line: Top of Knurr Formation.

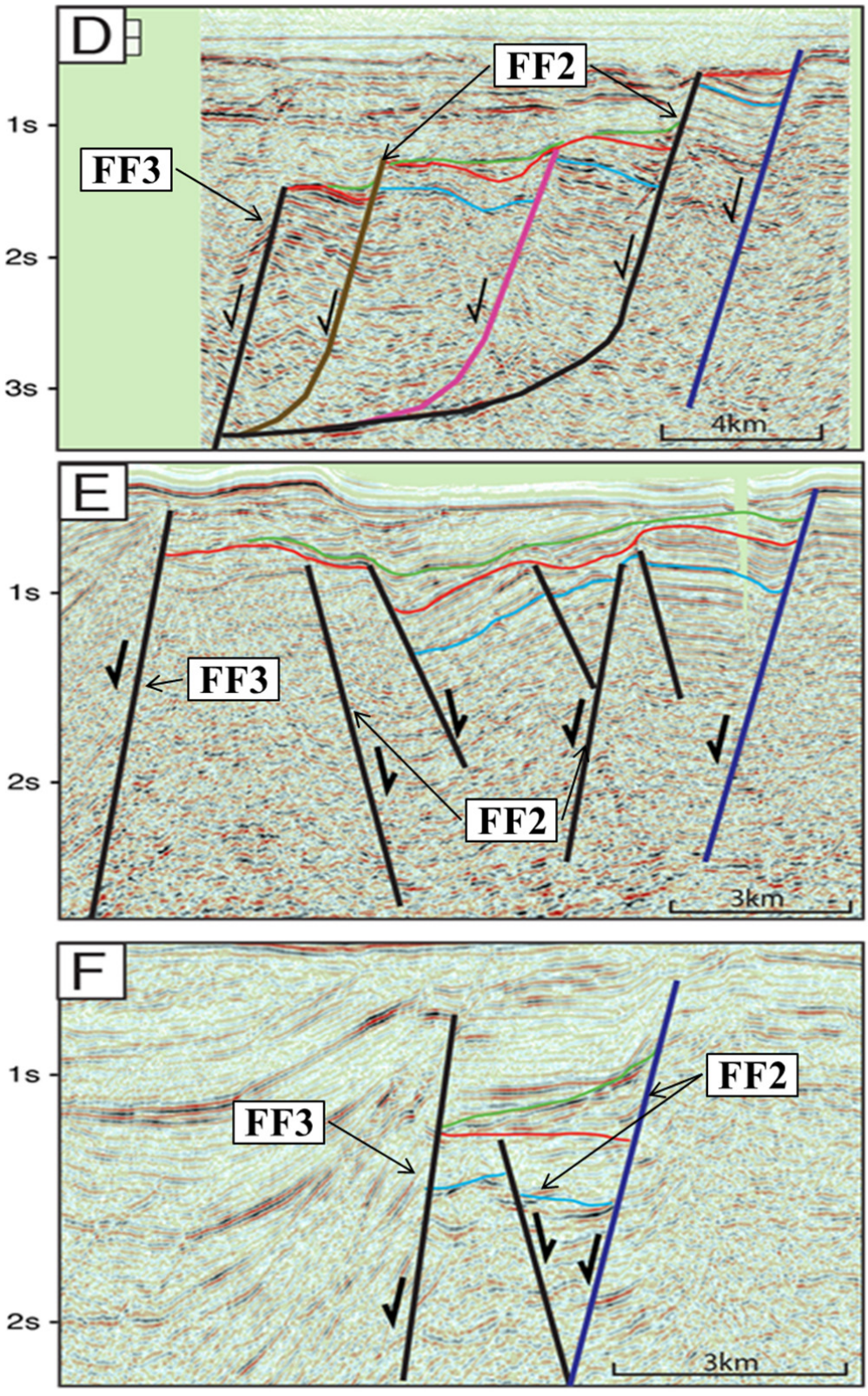

Fig. 20, Diplines D-F showing how the segmented structure is changing along strike. Blue line: Top of Stø Formation, Red line: BCU, Green line: Top of Knurr Formation. Note that lines E and F are 2D lines and have a smaller scale than the previous four lines from the 3D.

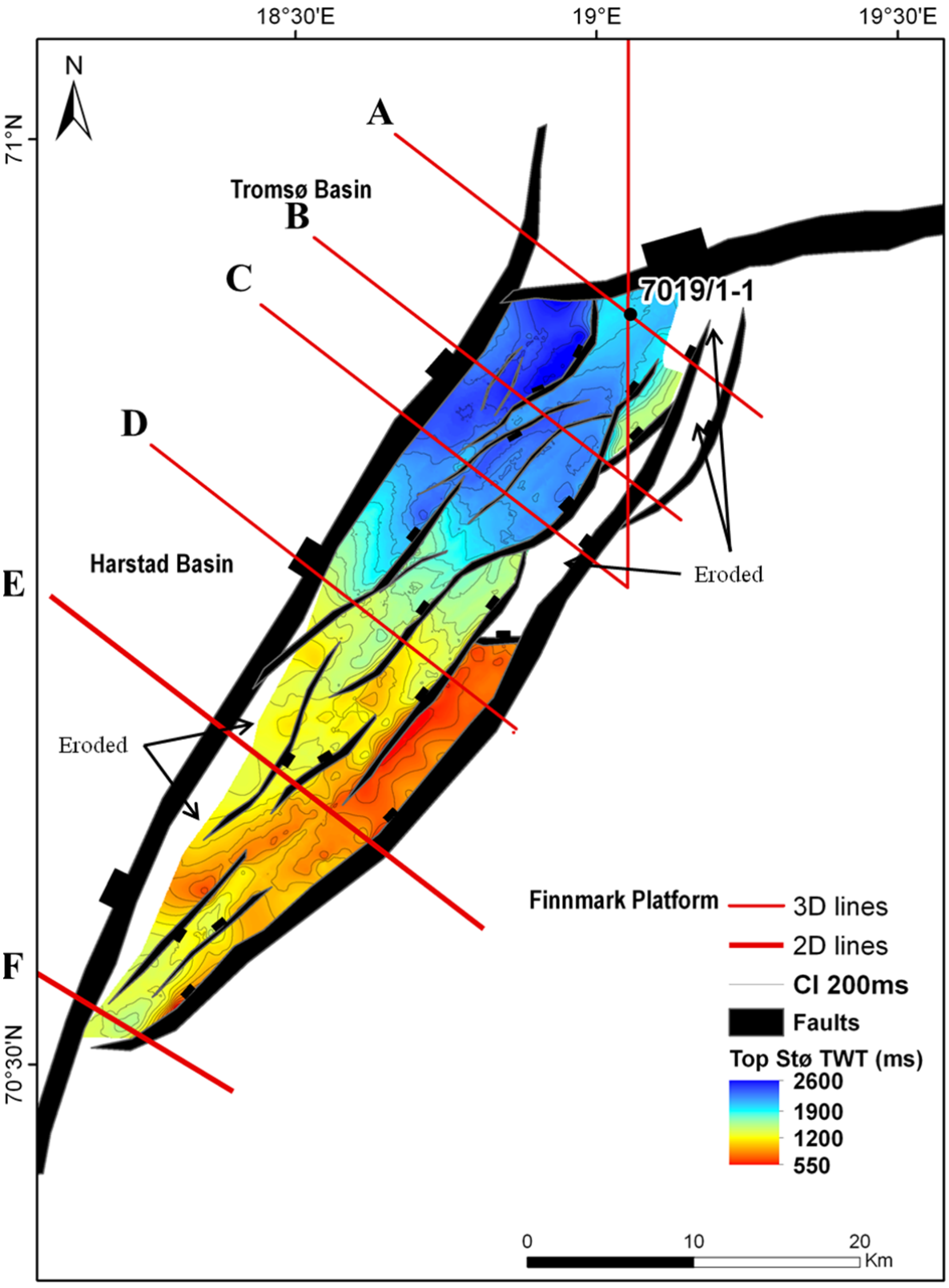

Fig. 21, Time structural map of the Top of Stø Formation, with the navigation of diplines A-F (Fig. 19, 20).

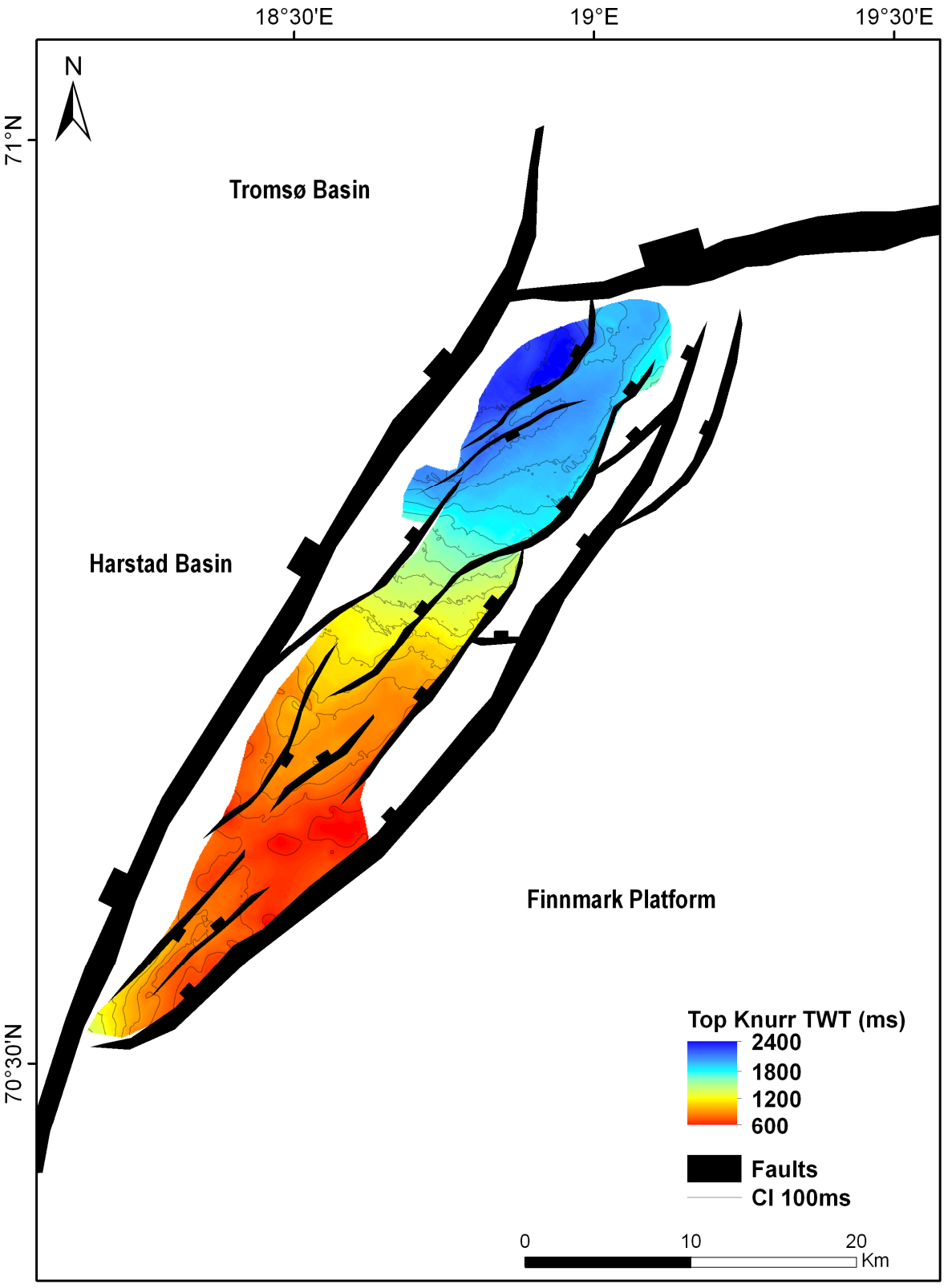

Fig. 22, Time structural map of the Top of Knurr Formation.

Seismic Characterization

Seismic Facies

Three seismic facies are recognized within the Lower Cretaceous syn-rift succession of the Knurr Formation. Table 2 shows a description of the seismic facies, characters and examples from the dataset. Three seismic lines (Fig. 23, 24, 25) along with seismic facies maps (Fig. 25) illustrate how the seismic facies are distributed relative to the faults.

Seismic Facies 1 (SF1) is identified adjacent to major faults of FF2. The reflection characters are chaotic to discontinuous, with low to high reflection amplitudes (Table 2). The SF1 are distributed lateral along adjacent major faults and is wedging towards the faults. SF1 is identified in three separate locations (SF1a, SF1b and SF1c) along the structure (Fig. 25, 26), and has a range of areas from 9-28km^2. The interpretation of SF1 is that they represent localized footwall sourced deposits, and that they are deposited orthogonal to the faults. Typical depositional elements in a deep marine setting sourced from adjacent faults are localized debris flows, debris flow aprons to faults scarp complexes. There is no well control on SF1, though debris flows are recognized in LF2. The lithology is highly related to the material that is being "slumped", and footwall collapses may contain blocks of Jurassic reservoir are be preserved in SF1. Recognition SF1 is highly depending on the orientation of the seismic line relative to the faults, and is best recognized in true diplines.

Seismic Facies 2 (SF2) is characterized by thicker packages of chaotic, transparent low amplitude reflections (Table 2). SF2 is situated on top of the erosional unconformity of BCU, and is locally ponded into minor sub-basins (grabens) onlapping the unconformable surface (Fig 24, 25). SF2 is located in the southern parts of the structure (Fig. 26) and represent an area of 104km^2. The interpretation of SF2 consists mainly of mudstones, with possible interbeds of siltstone similar to LF1. Depositional processes might be localized debris flows, and or mass transport complexes. SF2 can be identified in strike and diplines, and the paleodrainage is probably a mix of orthogonal and axial drainage. It seems to be sourced

orthogonal from the faults (Fig. 25), and then the direction has been changed in order to follow the strike of the faults towards north.

Seismic Facies 3 (SF3) is characterized by stacked continuous parallel high amplitude reflections (Table 2). SF3 has the largest scale of continuity, and is completely distributed across the structure, representing an area of 353km^2 (Fig. 26). Larger thicknesses of SF3 are likely to be preserved in the southern parts of the structure. Depositional processes seem to be characterized by fill and spill in and onlapping on top of BCU, SF1 and SF2 (Fig. 23, 24, 25). The interpretation of SF3 is that it represents turbiditic gravity flows to a submarine fan complex, containing sand rich lobes and channelized levees, sourced from feeder channels. The turbiditic events seem to be filling into the structure in an axial direction relative to the faults, and tilting of fault blocks will preserve sand rich channels closer towards adjacent faults.

Time thickness map

The time thickness map of the syn-rift (Fig. 27) is calculated from the BCU and the top of Knurr Formation and is indicating several thickness anomalies. The thickness variations of the syn-rift are preserved as elongated bodies along narrow grabens and wedges towards major faults. Wedges preserved along major faults seem to correlate with the distributions of SF1. The largest thicknesses are preserved in the southern part where larger depocenters have been generated. The distribution and larger accumulations are related to SF2 and SF3. Towards north and close to the well location, smaller thicknesses are forming wedges into a horst structure. Minor thickness variations of the Equal thicknesses and smaller variations of thickness seem to be related to filling and spilling of SF3.

Attribute map

RMS attribute map Fig. 28, calculated from the top of Knurr Formation surface, is showing minor amplitude anomalies which correspond to larger accumulation of the Lower Cretaceous, in particular towards the antithetic fault forming a horts, seen in the map ((Fig. 17), line B(Fig. 19).

Table 2, Summary of observations of main seismic facies identified in this study.

Seismic Facies	Seismic reflection characteristic	Scale	Interpretation	Examples
F1	Discontinous, chaotic, medium to high amplitude reflections	local, up to 1k from fault, 2-8km in width	Localized footwall sourced, fault scarp degradation complex to debris flow aprons, ortogonal	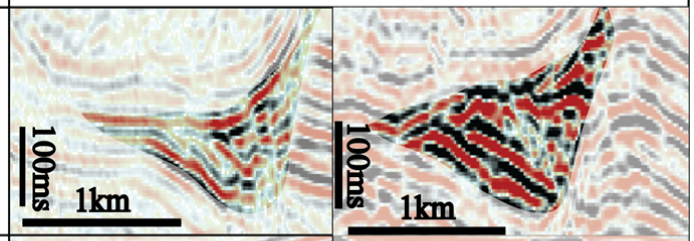
F2	Chaotic, continous low amplitude reflection	locally to sub regional 3-5km wide, 5-20km long	Debris flows to mass transport complex, axial and orthogonal	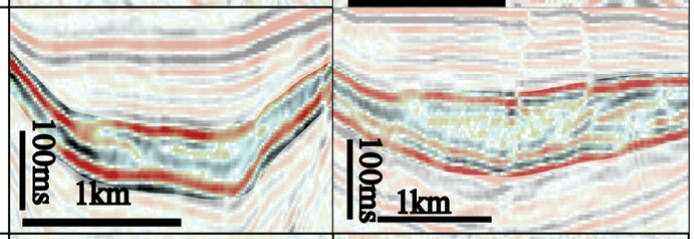
F3	Continous, high amplitude reflection	extensive 3-7km wide up to 40 km long	Turbidites, gravity flows, axially along the faults. Filling and spilling into the rotated fault blocks	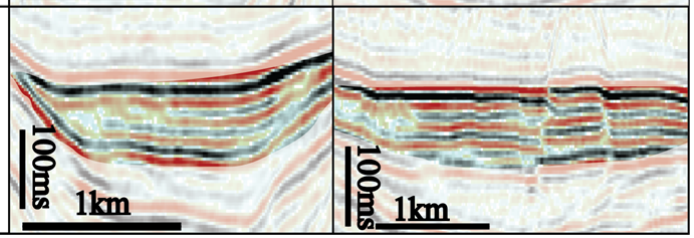

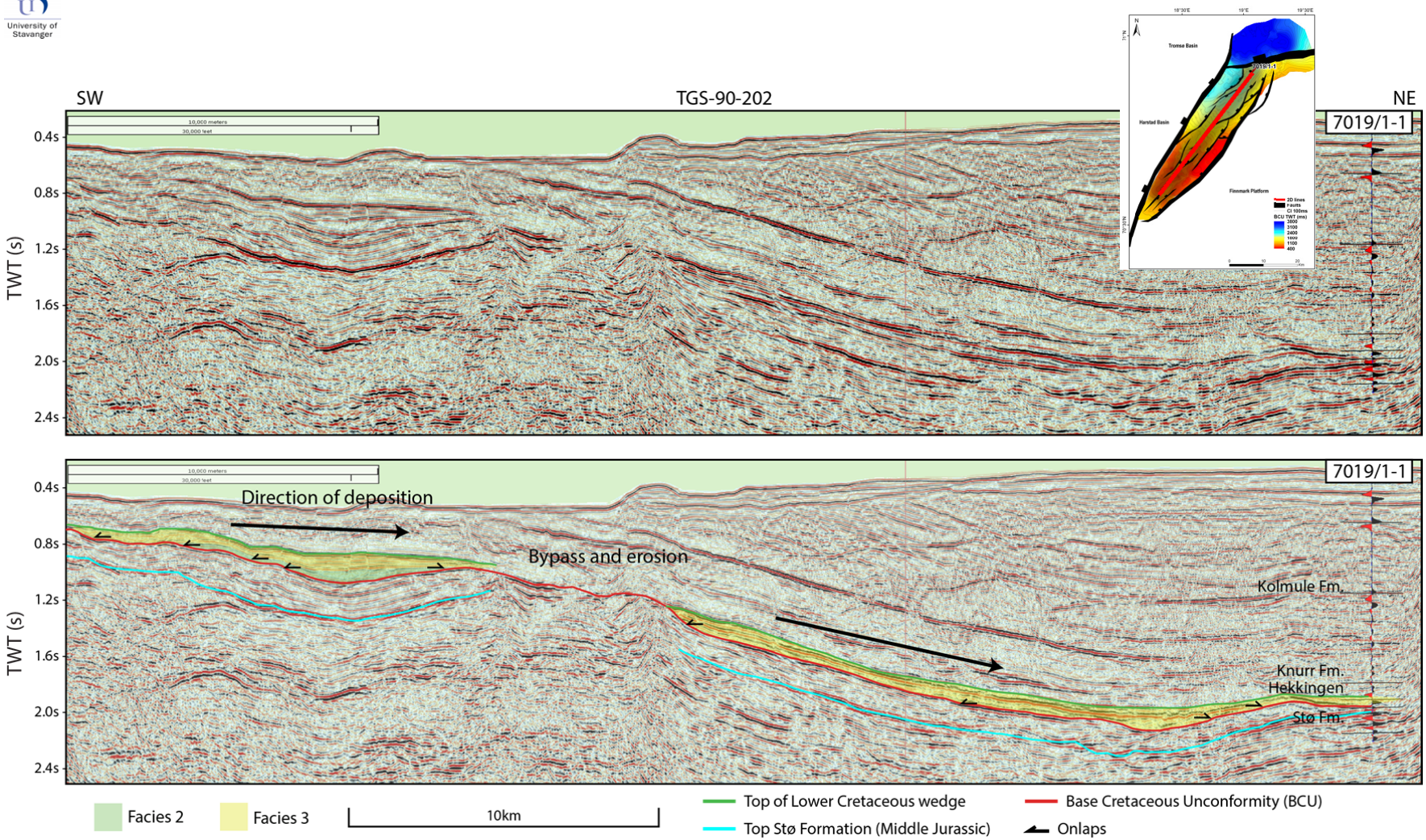

Fig. 23, Seismic 2D line TGS-90-202 along the strike of the wedge. Illustrating how the Lower Cretaceous wedge is filling and spilling towards north. Location of well 7019/1-1 is projected into the line.

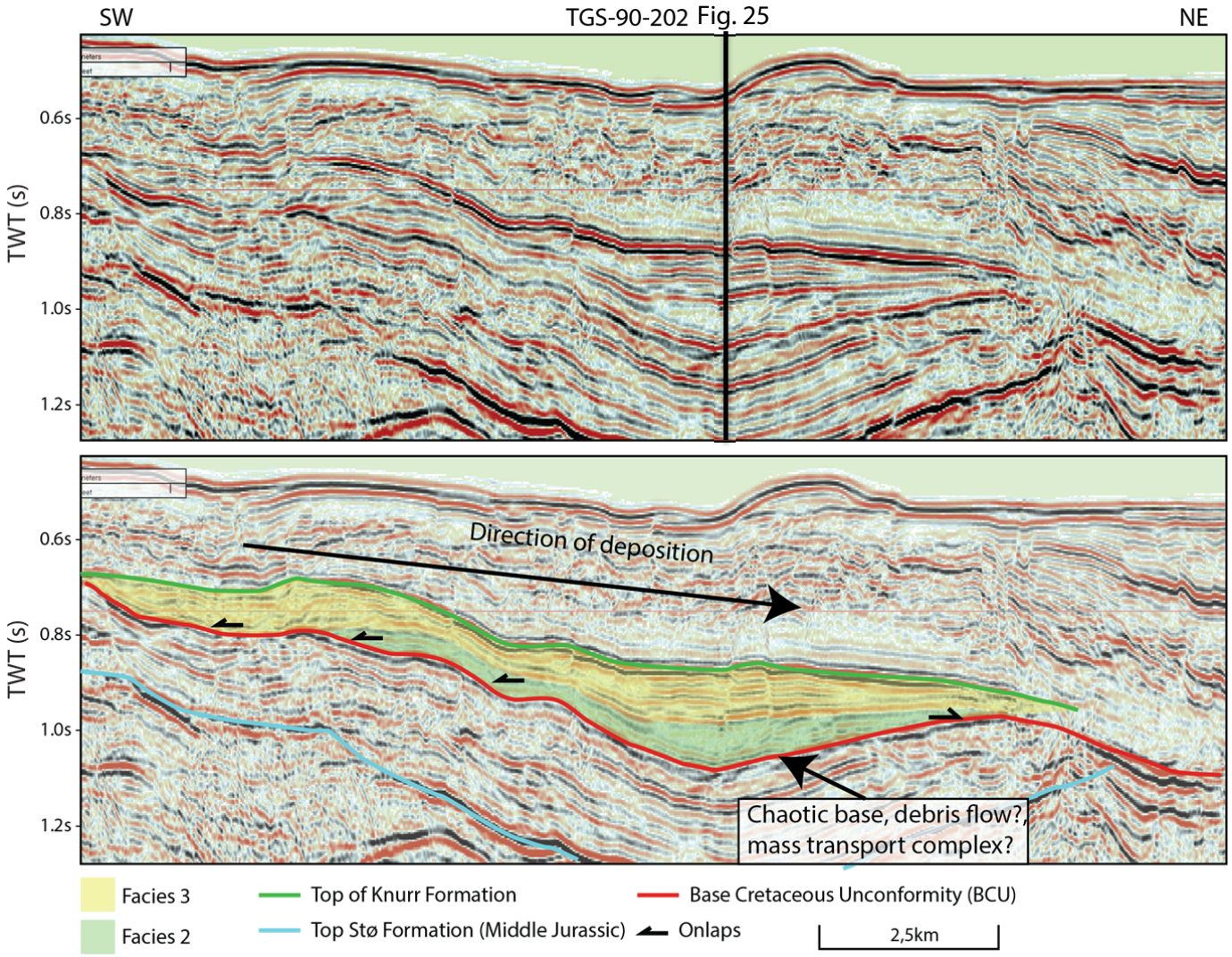

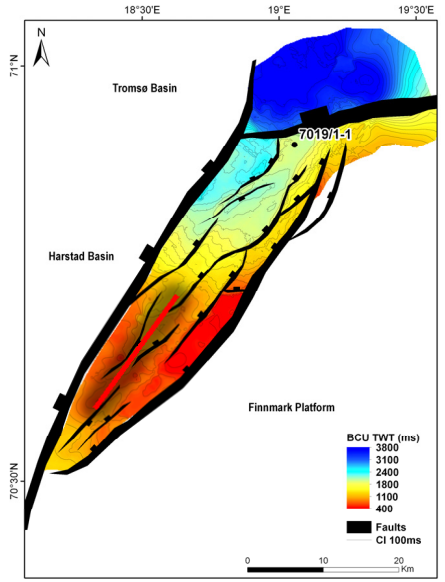

Fig. 24, closer look of the southern section of TGS-90-202, highlighting the identified seismic facies. Chaotic architecture of SF2 filling on top of BCU. SF3 is filling and spilling towards north. Navigation of Fig. 25 indicated by black vertical line.

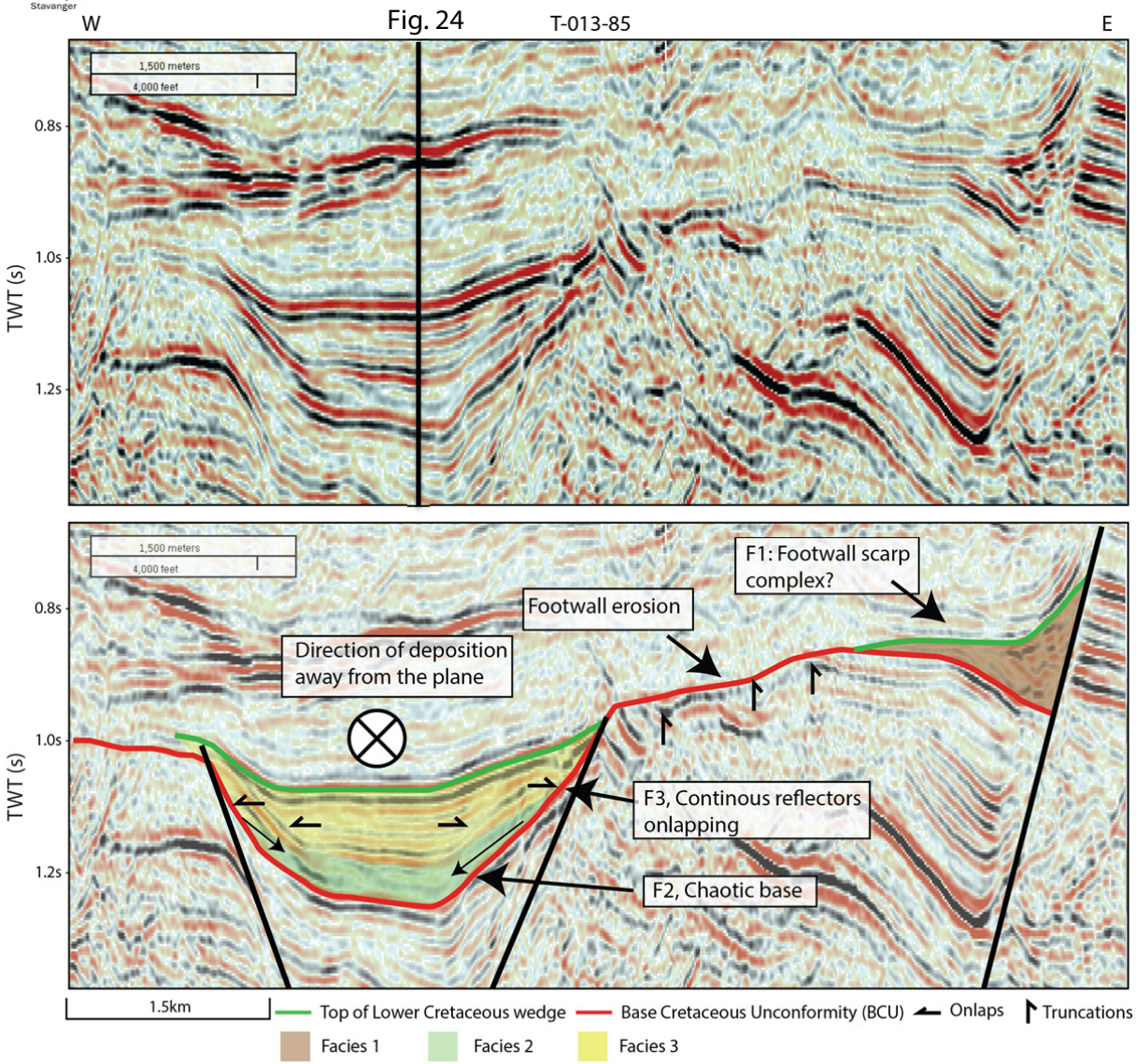

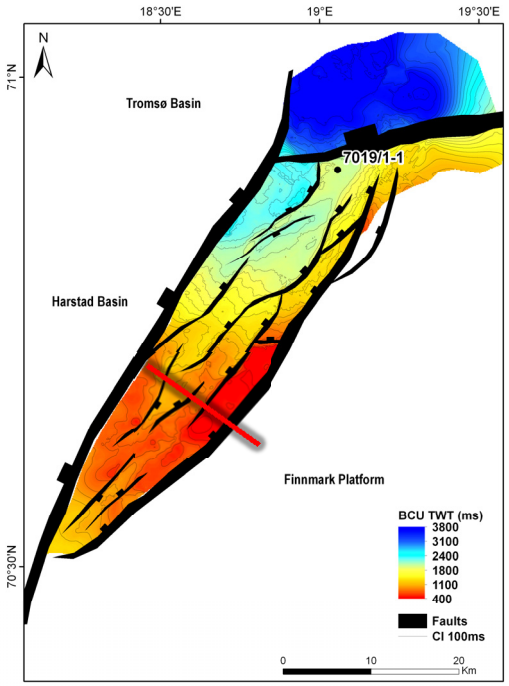

Fig. 25, Interpreted and uninterpreted dipline T-013-85, across the structure. SF1b is localized adjacent to a major fault. SF2 and SF3 are confined into a narrow graben onlapping BCU. Truncations of pre-rift Jurassic reflectors are indicating footwall erosion. SF2 may be sourced orthogonal from the adjacent footwall to the SE and the uplifted horst to the NW. SF3 is onlapping SF2 and BCU.

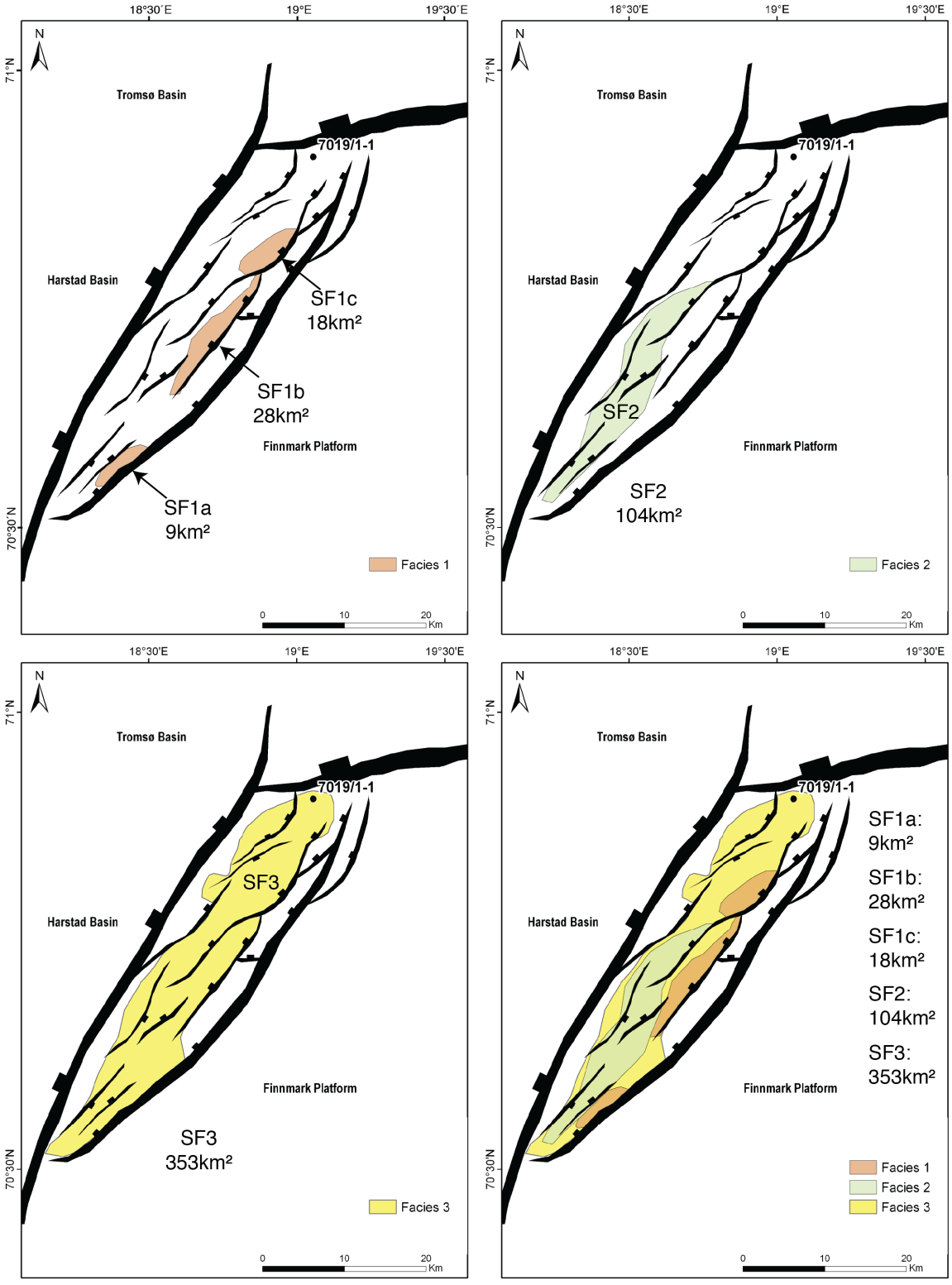

Fig. 26, Seismic facies maps illustrating the distribution of seismic facies, and their respective areal extent recognized in this study,

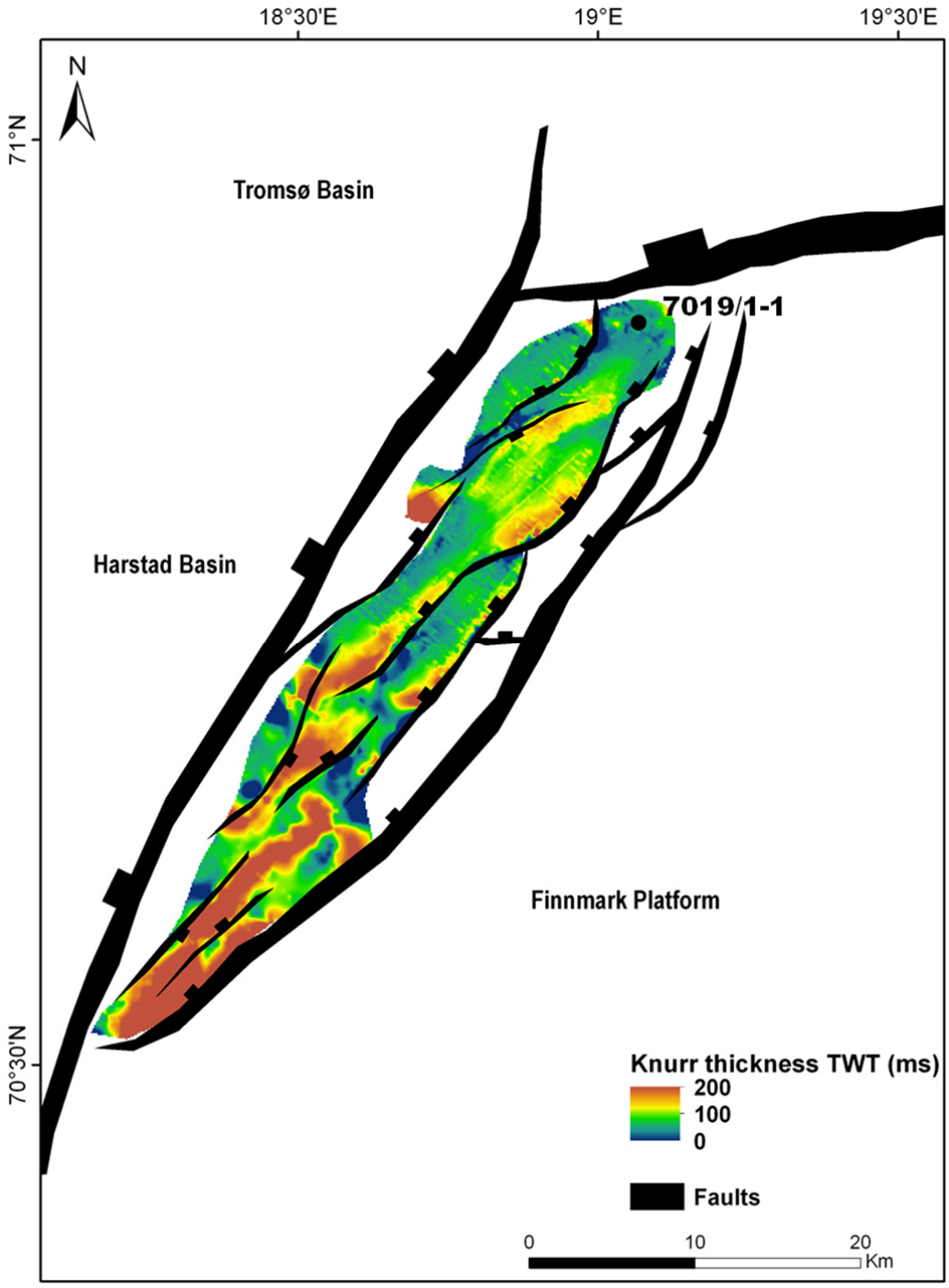

Fig. 27, Time thickness map of the Lower Cretaceous wedge (BCU-Top Knurr). Showing that the wedges are preserved as elongated bodies along the main rift axis, and are thickening towards the basin bounding faults.

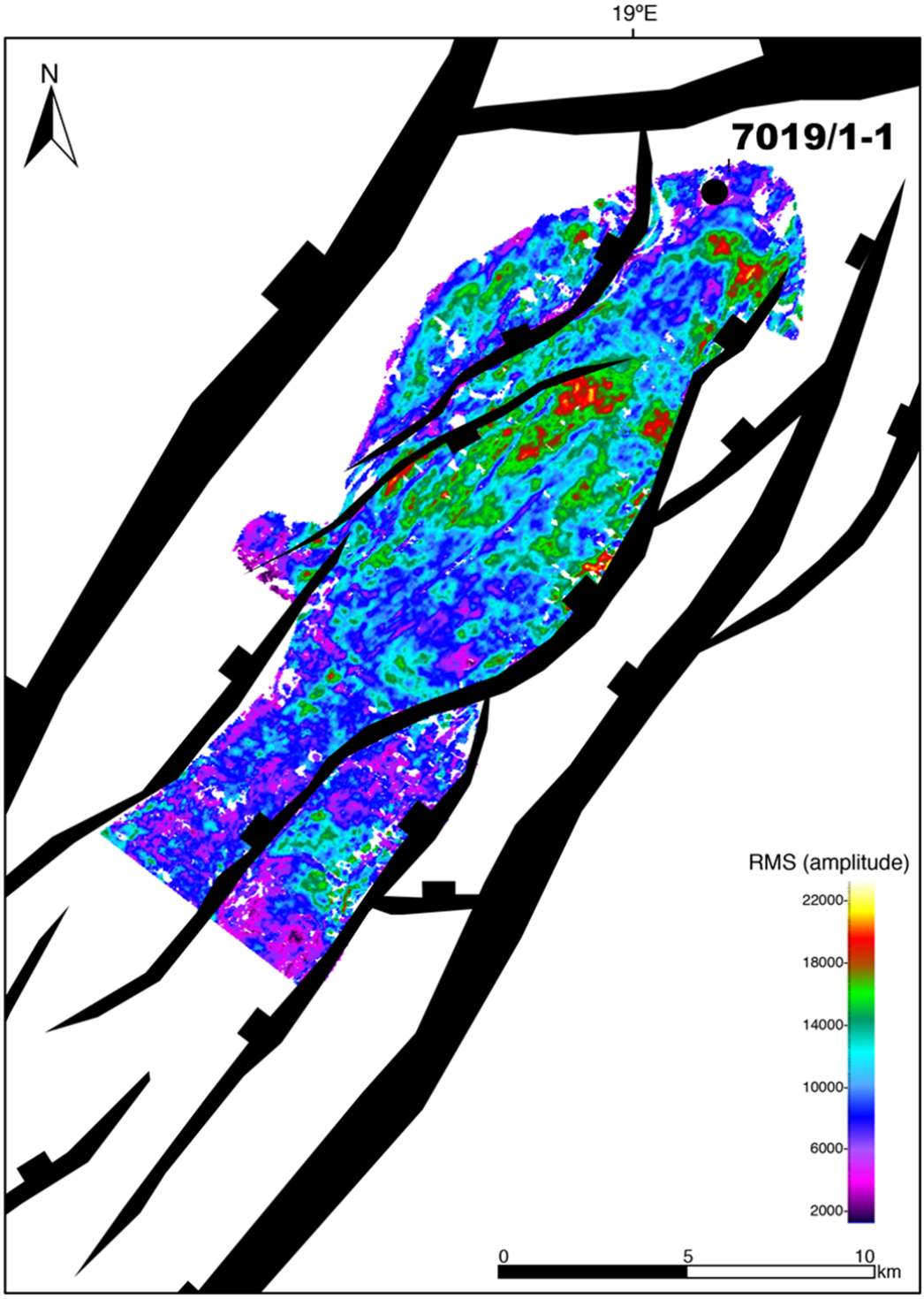

Fig. 28, Seismic attribute map, RMS. Minor anomalies of the attributes indicate thicker packages of the syn-rift.

DISCUSSION

Footwall uplift and control on paleodrainage

Fig. 30 is showing a 3D overview of the structure, illustrated with the BCU and with a surface of the seafloor on the Finnmark Platform, as the BCU is eroded and not present. The three main fault families (Fig. 29) are confining the segmented structure. The large scale flexural footwall uplift the interaction between the three large faults (Fig. 30) seems to control the paleodrainage into the structure. The large scale flexural uplift of FF1 towards north is making a barrier with the footwall in the north and control sediment dispersal away from FF1 (Fig. 29, 30). Similarly the large flexural uplift of FF3 is controlling the sediment dispersal from the southwest routing sediments towards north. Flexural uplift of FF2 (blue fault in Fig.29) seem to control the paleodrainage sourced from the Finnmark Platform and mainland Norway. Fluvial systems may have been deflected away from the uplifted footwall of FF2 and around the tips of the faults and acting as single point feeder systems, with entry points to the south and possibly to the north (Fig. 30). In the smaller scale, the distribution and paleodrainage of the seismic facies seems to be controlled by the smaller fault of FF2. The depocenters created by FF2 are catching sediment routed into the structure, and controlling the distribution of sediment in the segmented terrace. The structure gets progressively deeper towards northwest (Fig. 29, 30) and there might be a spill point towards the Tromsø Basin in this area.

Structural Evolution of FF2

The Stø Formation (fig. 21) represents the pre-rift stage of FF2. Interpretation of the Stø Formation shows that the surface is a lot more segmented (Fig. 19, Fig. 20 lines B-F) with faults that are not affecting the BCU. These faults were active during an early stage of the rifting period, similar to the initiation stage (Fig. 9, 10). As rifting continues, larger faults are linking up and the minor faults are becoming inactive (similar to fault Y and Z in Fig. 10). The BCU surface (Fig. 17) is generally offset by larger faults, and not by the smaller faults that affected the pre-rift. The larger faults of FF2 which is offsetting the BCU, is generating the major depocenters along the axis of the structure. The Knurr Formation surface (Fig. 22) is confined along the faults of FF2 which forms the depocenters. The top of the surface is generally not faulted and represents the late syn-rift to post-rift stage of the evolution of FF2.

Evolution of Lower Cretaceous wedges in the TFFC

Stage 1: The first stage represents a mix of SF1 and SF2, the seismic facies does not over each other and they seem to occur syn-tectonically. The distribution of SF1 and SF2 are controlled and confined by the faults of FF2 (Fig. 31). The debris flows interpreted for SF1 and SF2 are illustrated in (Fig. 32), and shows how they are distributed adjacent to the faults. Where SF1 represent localized footwall sourced deposition and SF2 are representing muddy debris flows sourced in an axial direction.

Stage 2: SF3 is onlapping parts of SF2 and completely over SF2 and has to be older than SF2, and it may occur syn-tectonically with SF1. SF3 is distributed over the whole structure and the paleodrainage of SF3 seems to be controlled by the footwall uplift and interaction of the three major faults (Fig. 29). The turbidites interpreted in SF3 are illustrated in (Fig. 32) showing how turbiditic lobes sourced from a proximal location in the south might prograde and spill into the structure, around tips of faults and into relay ramps (Fig. 31).

Sediment sources

Erosion of the Stø Formation, which contains clean sandstones (Fig.16), is a good candidate for the source of the Lower Cretaceous massive, non-graded sandstones (LF3, Table 1). Seldal (2005) pointed out that provenance studies of the Lower Cretaceous sediments in well 7019/1-1 were derived from Middle Jurassic and Permian rocks, and it is highly likely that these sediments are sourced from the uplifted Finnmark Platform in the southeast. The development of a mature clastic system on the shelf might be the main source of the turbiditic sandstones identified in SF3. The IKU well 7018/5-U-1(Fig. 31) contains a condensed section of the Klippfisk Formation. The well location of 7018/5-U-1 is situated on the footwall of the structure on the Finnmark Platform. The Klippfisk Formation represents condensed carbonates, limestones and marls deposited shallow marine transgressive environments (Smelror et al., 1998; Smelror et al., 2001). The Formation and is time equivalent (Berriasian to Early Barremian) to the Knurr Formation, and the condensed nature of the formation and missing sections might reveal times of subaerial exposure indicating exposure of the proximal shelfal areas adjacent to the structure.

The conceptual model of the syn-tectonic depositional environments of the Knurr Formation (Fig. 32) is showing the depositional environments in the deep marine settings might have been.

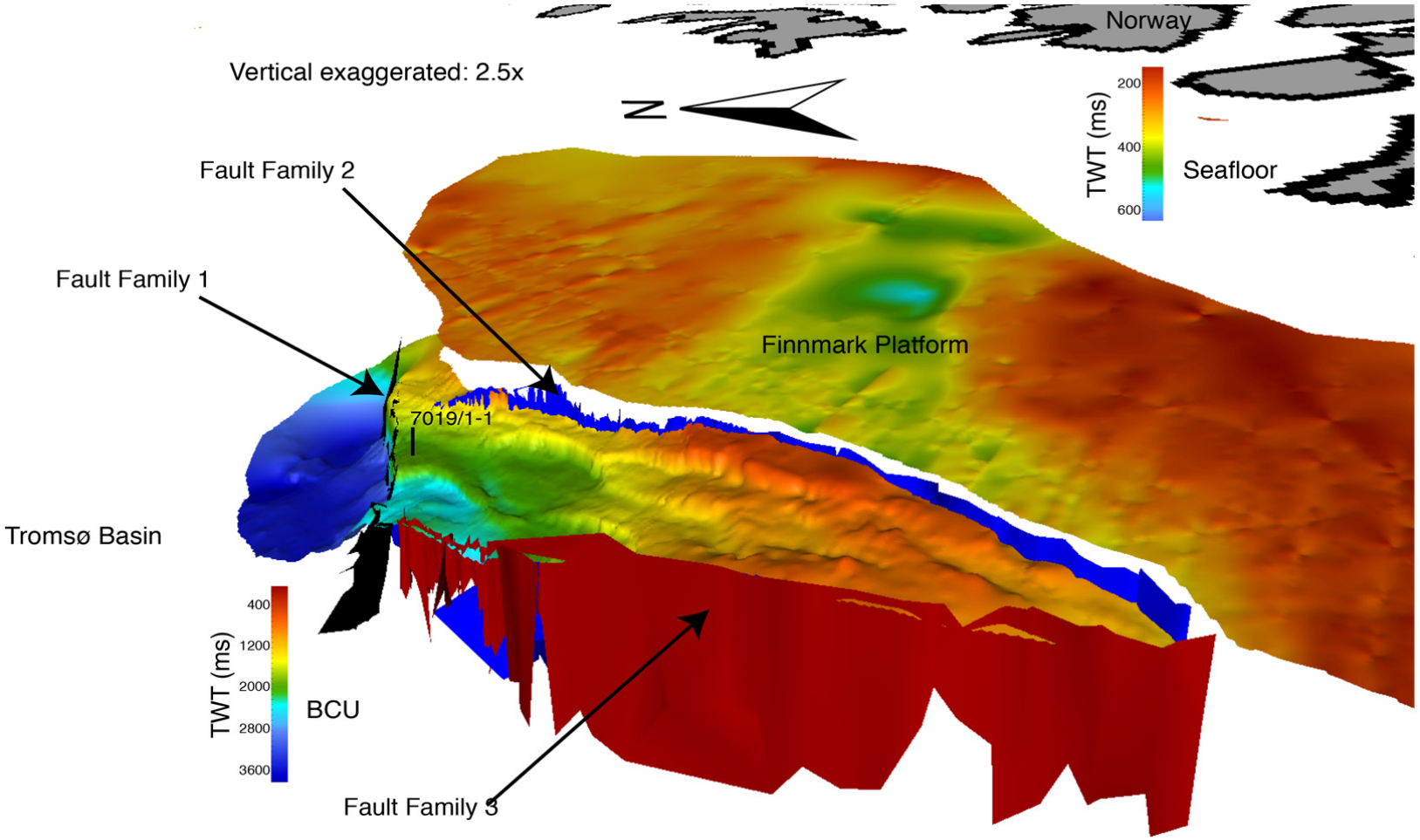

Fig. 29, 3D overview of the structure. Looking towards east, the coastline of Finnmark is in the top right. The structure is projected by the base Cretaceous unconformity with the well location in the north. On the Finnmark Platform ,a map of the seafloor is projected, representing the unconformity at the Finnmark platform, as the BCU is eroded. The three main fault families are indicated by arrows. Notice how the structure gets deeper towards the north.

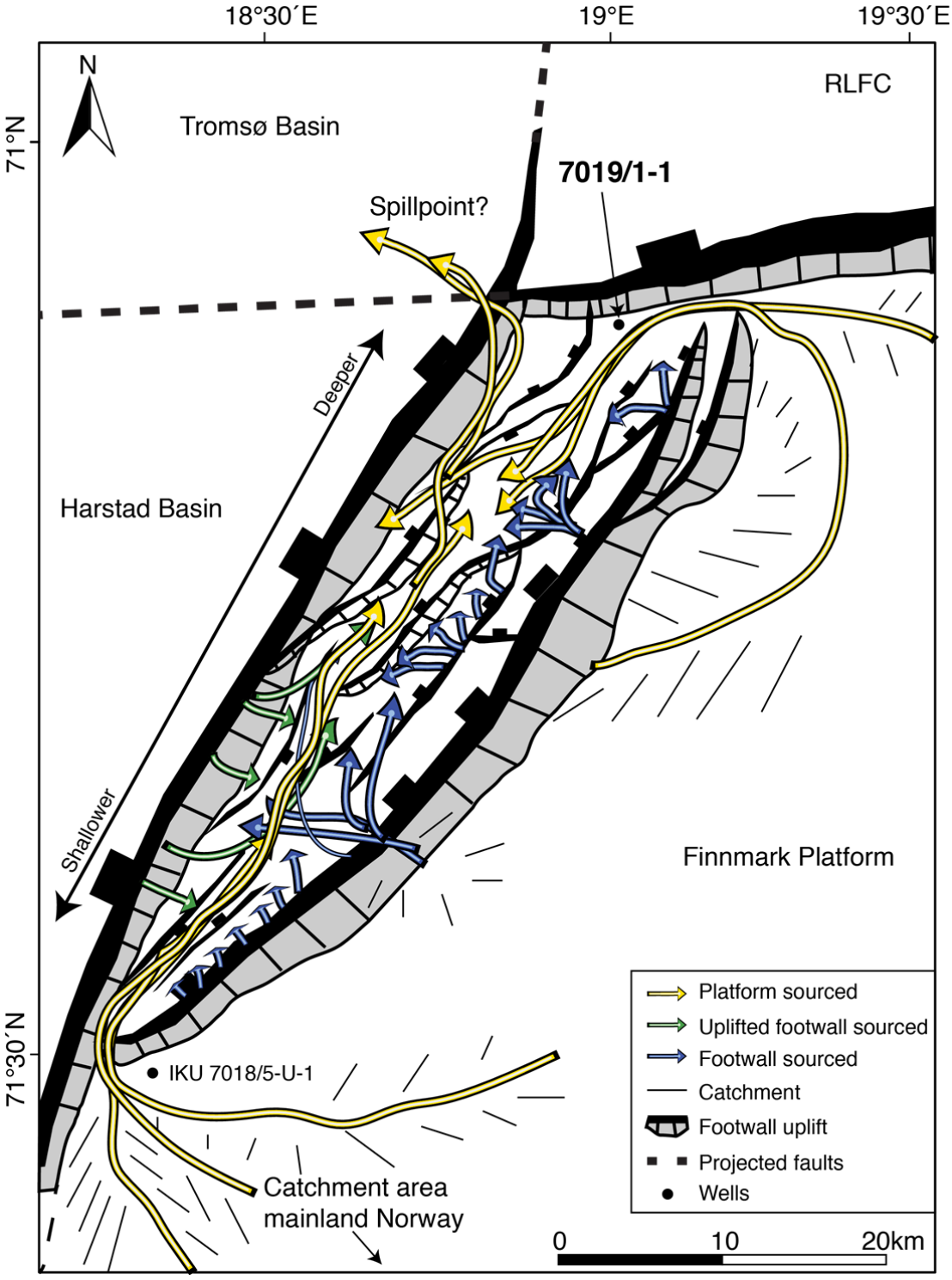

Fig. 30, Proposed map of the paleodrainage of the syn-rift succession during Lower Cretaceous. The flexural footwall uplift of the three main faults will confine the catchment area for preserving the sediments. The structure has a relief towards northwest.

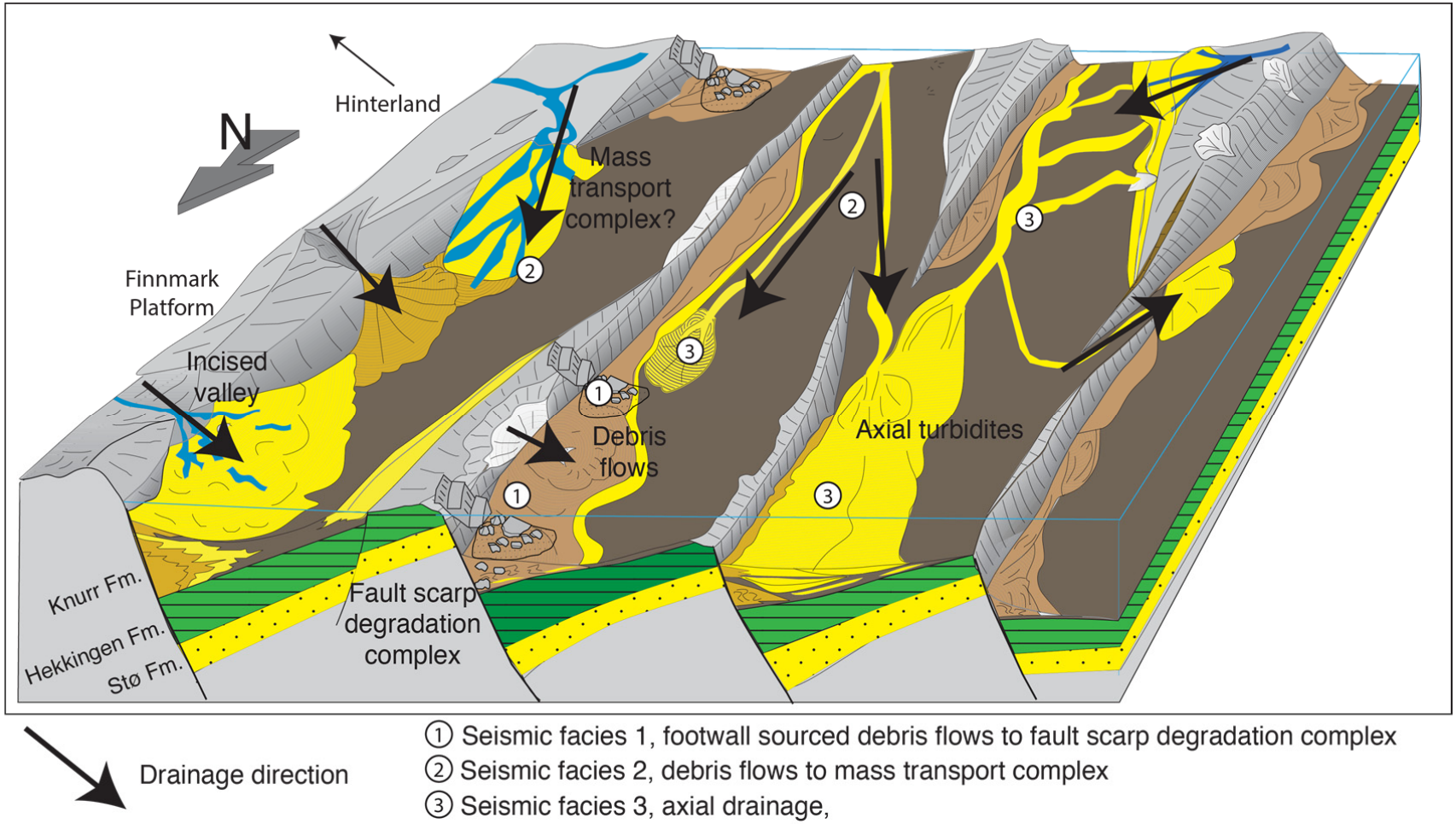

Fig. 31, Conceptual model, illustrating the syn-tectonic depositional processes proposed during Lower Cretaceous in the study area. Identified seismic facies is annotated in the figure. Modified from (Ravnas and Steel, 1998)

Seismic facies and grain size distribution vs. slope gradients

SF1 and SF2 are distributed more locally compared to SF3. If SF3 is sourced from the Finnmark Platform in the south (Fig. 30), how is the sands able to prograde all the way to the well location? Depending on the relief of a slope and grain size, how far are sediments able to travel? (Reading and Richards, 1994) classifies turbiditic systems in deep-water basins, and are separating them based on how different feeder systems might contribute to the sediment dispersal in a deep marine setting. A simple calculation of the slope gradients in line TGS-90-202 (Fig.32) shows a slope gradient of the structure in the range 36-42m/km. This matches the range for sand prone submarine fans, sourced from a single point with a radius from 10-100km. The range matches well with the interpretation of SF3, and the fact that SF3 was penetrated by well 7019/1-1 it is likely to assume that better reservoirs can be preserved in more proximal positions away from the well (Fig. 29). The radius range for a single point sourced submarine gravel fan comes in the range of 1-50km, has smaller catchment, and matches well with the interpretation of SF1 (Table 2 and Fig. 26).

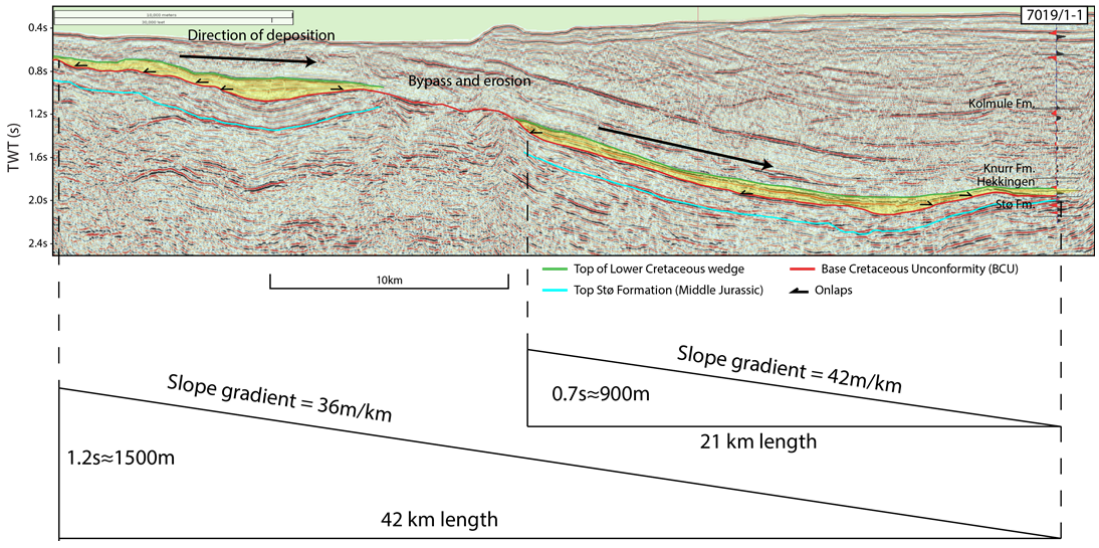

Fig. 32, Slope gradients calculated from Line TGS-90-202, showing the relief of the drainage towards the well location in the north, location of line in fig.23.

Petroleum potential

Field analogues

In the Moray Firth Basin offshore United Kingdom in the North Sea, there are several fields and discoveries in Lower Cretaceous syn-rift plays. One of these is the Britannia Field (Fig. 33) (Copestake et al., 2003), where clastic wedges are developed along the basin margins of uplifted highs. The Britannia Field, consists mainly of the Britannia Sandstone Formation, and is aged from Barremian to Aptian. Several processes of sedimentation are present, and typical lithofacies are high density turbidites to more muddy debris flows, (Fig.33). Well correlation across the field shows how the sands are pinching out from proximal towards distal depositions. If the well 7019/1-1 is situated in a distal part of a turbiditic system (Fig. 34), there is large upside for better reservoirs qualities towards a proximal part of the system. The turbiditic lobes will be better developed into amalgamated turbiditic sand complexes, the net sand will be higher and the reservoir properties will be higher. The Britannia field is compared to the interpreted structure (Fig. 35) to make an impression of the size.

Reservoir potential

Well 7019/1-1 encountered 52m of net sand with an N/G of approximately 0.42, with average porosities of the reservoirs to be 13%. (Halland et al., 2014), may imply that the properties of the Lower Cretaceous reservoirs were better than the Middle Jurassic reservoirs, which had experienced more diagenesis and stylolitilization. It is well known that the Barents Sea has experienced large scale Cenozoic uplift and erosion, and the burial history of the Barents Sea has great impact on the petroleum system (Henriksen et al., 2011). Net erosion estimations from (Henriksen et al., 2011) indicates that the maximum burial for the Jurassic reservoirs in well 7019/1-1 is around 3100m which gives a net erosion of around 600m (Fig. 36). Reservoir targets further south, where the structure is shallower (Fig. 29), has probably experienced less burial and it is likely to find better reservoir properties.

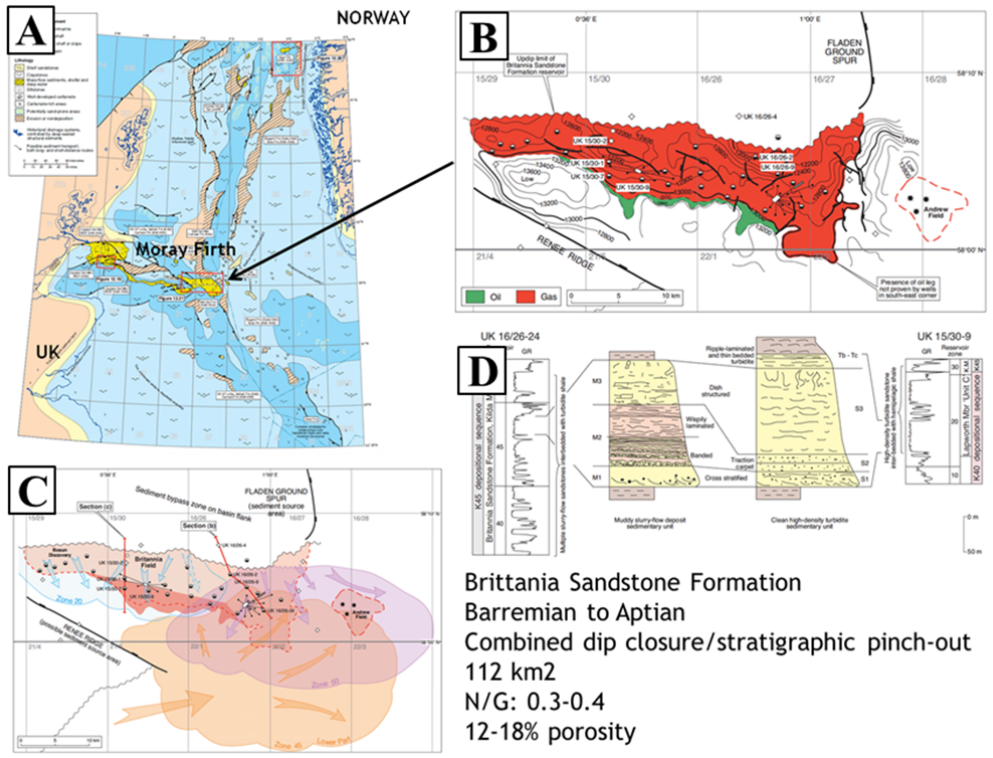

Fig. 33 Britannia Field UK, A: Location of the Britannia Field in the Moray Firth Basin offshore UK in the North Sea. B: Size of the Britannia Field, with hydrocarbon contacts. C: Arrows are indicating several sources of sedimentation and paleodrainage. D: Samples of typical lithofacies found in the Britannia Field. (Copestake et al., 2003)

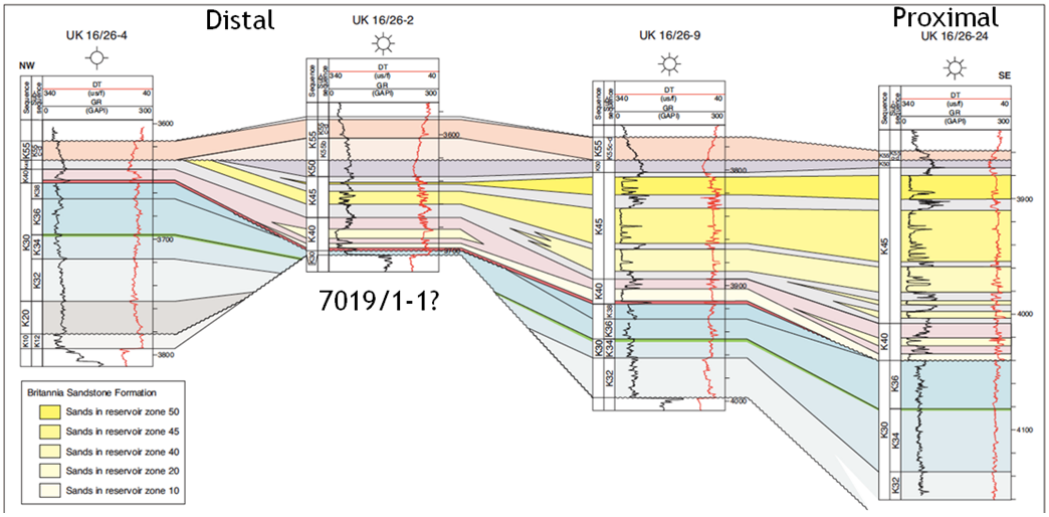

Fig. 34, Wells from the Britannia Field, illustrating how the turbiditic sands are pinching out from proximal to distal. If well 7019/1-1 is situated in a distal part of a turbiditic system, there remains a large potential for better reservoirs proximal. (Copestake et al., 2003)

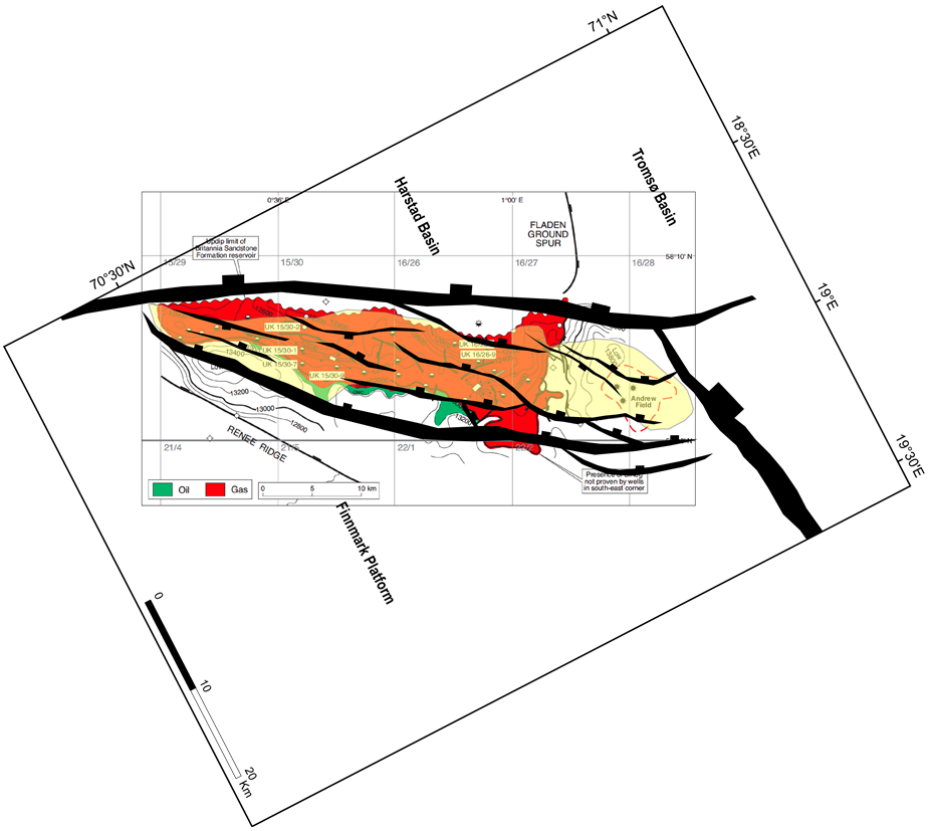

Fig. 35, Size comparison of the Britannia Field compared to the study area.

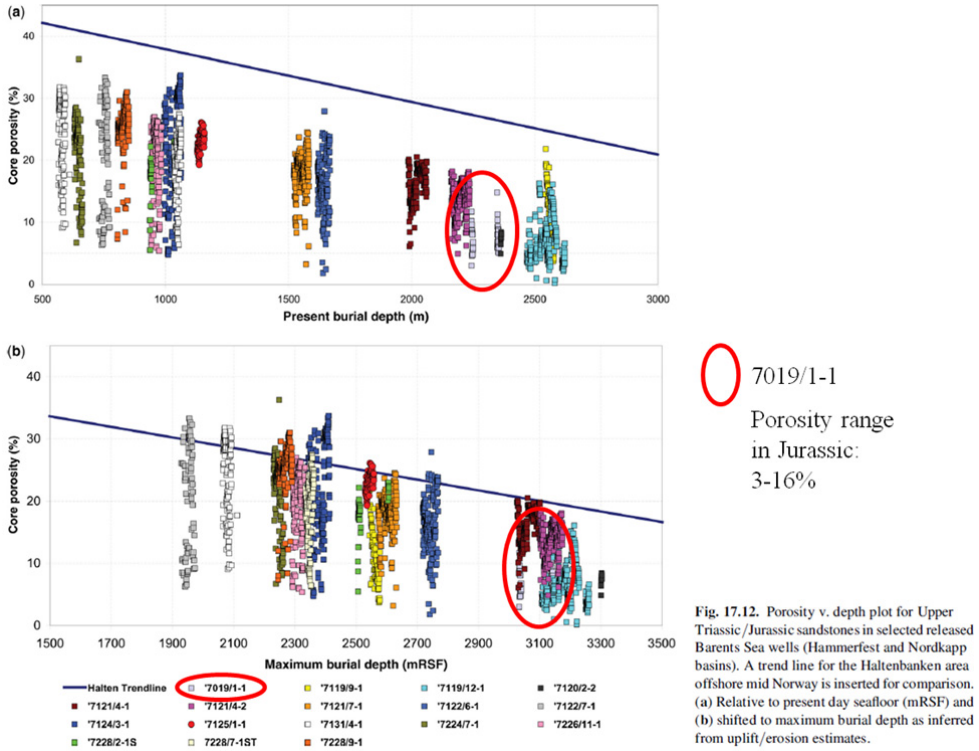

Fig. 17.12. Porosity v. depth plot for Upper Triassic/Jurassic sandstones in selected released Barents Sea wells (Hammerfest and Nordkapp basins). A trend line for the Haltenbanken area offshore mid Norway is inserted for comparison. (a) Relative to present day seafloor (mRSF) and (b) shifted to maximum burial depth as inferred from uplift/erosion estimates.

Fig. 36, Porosity vs. depth chart from Henriksen et al. (2011), comparing present day burial (top) and maximum burial depth (bottom). The core porosity data points in well 7019/1-1 are calculated in the Jurassic sandstones.

Seismic resolution and limitations

The low frequency resolution of the 3D seismic data mentioned in the data quality (Fig. 14, 15) will have a great impact on defining stratigraphic closures. The low vertical resolution may be sufficient for structural interpretation, but it will be limited in use for defining stratigraphic traps. Reprocessing of the 3D seismic data by increasing the frequency spectrum is highly recommended. The reprocessed seismic data could be inverted by the use of the well 7019/1-1. AVA analysis of new inverted 3D seismic may reveal possible stratigraphic traps within the Knurr Formation.

CONCLUSIONS

i. The three main fault families are confining the terrace, and controlling the paleodrainage of the Lower Cretaceous wedges. The flexural uplift of FF1 and FF3 confines the paleodrainage into the structure and the smaller faults ofFF2 is controlling the distribution of sediment dispersal.

ii. Rotation of fault blocks with SW-NE faults of FF2 develop along strike sediment depocenters, and can be characterized by fill and spill processes.

iii. The wedges can be characterized based on their seismic characters and are showing chaotic high amplitudes (SF1), chaotic low amplitude (SF2) to continuous high amplitude reflections (SF3), in which one can be correlated with well data.

iv. The main lithofacies identified core, consists of heterolithic mudstones, debris flows and high density turbidites, and can be correlated with SF3

v. Footwall sourced sediments are characterized from SF1 and SF2.

vi. The Finnmark Platform which was subaerial exposed during Lower Cretaceous has been acting as a large source of sediments, and sediments are point sourced into the structure from the exposed platform.

vii. The potential for good quality reservoirs is probable higher further south on the structure, where the system identified in SF3 seems to be better developed.

viii. Large analogous fields in Lower Cretaceous plays in the North Sea are indicating the potential that remains. Lower Cretaceous wedges may be important future targets in the Barents Sea.

REFERENCES

Breivik, A.J., Faleide, J.I. and Gudlaugsson, S.T. (1998) Southwestern Barents Sea margin: late Mesozoic sedimentary basins and crustal extension. *Tectonophysics*, **293,** 21-44.

Chopra, S., Castagna, J. and Portniaguine, O. (2006) Seismic resolution and thin-bed reflectivity inversion. *CSEG recorder*, **31,** 19-25.

Copestake, P., Sims, A., Crittenden, S., Hamar, G., Ineson, J., Rose, P. and Tringham, M. (2003) Lower Cretaceous. *The Millennium Atlas: petroleum geology of the central and northern North Sea***,** 191-211.

Dalland, A., Worsley, D. and Ofstad, K. (1988a) *A Lithostratigraphic Scheme for the Mesozoic and Cenozoic and Succession Offshore Mid-and Northern Norway*. Oljedirektoratet.

Dalland, A., Worsley, D. and Ofstad, K. (1988b) A lithostratigraphic scheme for the Mesozoic and Cenozoic succession offshore Norway north of 62 N. *NPD Bull*, **4,** 67.

Faleide, J.I., Tsikalas, F., Breivik, A.J., Mjelde, R., Ritzmann, O., Engen, Ø., Wilson, J. and Eldholm, O. (2008) Structure and evolution of the continental margin off Norway and the Barents Sea. *Episodes*, **31,** 82-91.

Faleide, J.I., Vågnes, E. and Gudlaugsson, S.T. (1993) Late Mesozoic-Cenozoic evolution of the south-western Barents Sea in a regional rift-shear tectonic setting. *Marine and Petroleum Geology*, **10,** 186-214.

Gabrielsen, R. (1984) Long-lived fault zones and their influence on the tectonic development of the southwestern Barents Sea. *Journal of the Geological Society*, **141,** 651-662.

Gawthorpe, R.L. and Leeder, M.R. (2000) Tectono-sedimentary evolution of active extensional basins. *Basin Research*, **12,** 195-218.

Gradstein, F.M., Anthonissen, E., Brunstad, H., Charnock, M., Hammer, O., Hellem, T. and Lervik, K.S. (2010) Norwegian Offshore Stratigraphic Lexicon (NORLEX). *Newsletters on Stratigraphy*, **44,** 73-86.

Grundvåg, S.-A. and Olaussen, S. (2013) The offshore-onshore link of Lower Cretaceous clastic wedges in the Barents Sea and Svalbard: a tool for risk mitigation of plays. In: *AAPG 3P Arctic Conference and Exhibition: The Polar Petroleum Potential*, Stavanger, Norway.

Grundvåg, S.-A., Olaussen, S., Jelby, M.E., Sandvik, S.E. and Aadland, T. (2014) An integrated approach for improving the understanding of Lower Cretaceous clastic wedges in the Barents Sea: new observations from outcrop and subsurface studies in Svalbard. In: *NGF Arctic Conference Days: Arctic Energy*, Tromsø.

Halland, E.K., Mujezinović, J. and Riis, F. (2014) CO2 Storage Atlas Norwegian Continental Shelf. *Norwegian Petroleum Directorate*.

Henriksen, E., Bjørnseth, H.M., Hals, T.K., Heide, T., Kiryukhina, T., Kløvjan, O.S., Larssen, G.B., Ryseth, A.E., Rønning, K., Sollid, K. and Stoupakova, A. (2011) Chapter 17 Uplift and erosion of the greater Barents Sea: impact on prospectivity and petroleum systems. *Geological Society, London, Memoirs*, **35,** 271-281.

Jackson, C.A.-L., Barber, G.P. and Martinsen, O.J. (2008) Submarine slope morphology as a control on the development of sand-rich turbidite depositional

systems: 3D seismic analysis of the Kyrre Fm (Upper Cretaceous), Måløy Slope, offshore Norway. *Marine and Petroleum Geology*, **25,** 663-680.

Leeder, M.R. and Jackson, J.A. (1993) The interaction between normal faulting and drainage in active extensional basins, with examples from the western United States and central Greece. *Basin Research*, **5,** 79-102.

Mosar, J., Torsvik, T. and Team, B. (2002) Opening of the Norwegian and Greenland Seas: Plate tectonics in mid Norway since the Late Permian. *BATLAS– Mid Norway Plate Reconstruction Atlas with Global and Atlantic Perspectives***,** 48-59.

NPD 2013. The petroleum resources on the Norwegian continental shelf, Norwegian Petroleum Directorate, Norwegian Petroleum Directorate.

Prosser, S. (1993) Rift-related linked depositional systems and their seismic expression. *Geological Society, London, Special Publications*, **71,** 35-66.

Ravnas, R. and Steel, R.J. (1998) Architecture of marine rift-basin successions. *AAPG Bulletin*, **82,** 110-146.

Reading, H.G. and Richards, M. (1994) Turbidite systems in deep-water basin margins classified by grain size and feeder system. *AAPG Bulletin*, **78,** 792-822.

Riis, F., Vollset, J. and Sand, M. (1986) Tectonic development of the western margin of the Barents Sea and adjacent areas.

Rønnevik, H. and Jacobsen, H.-P. (1984) *Structural highs and basins in the western Barents Sea*. Springer.

Seldal, J. (2005) Lower Cretaceous: the next target for oil exploration in the Barents Sea? *Geological Society, London, Petroleum Geology Conference series*, **6,** 231-240.

Smelror, M., Mørk, A., Monteil, E., Rutledge, D. and Leereveld, H. (1998) The Klippfisk formation - a new lithostratigraphic unit of Lower Cretaceous platform carbonates on the Western Barents Shelf. *Polar Research*, **17,** 181-202.

Smelror, M., Mørk, A., Mørk, M.B.E., Weiss, H.M. and Løseth, H. (2001) Middle jurassic-lower cretaceous transgressive-regressive sequences and facies distribution off northern nordland and troms, Norway. In: *Norwegian Petroleum Society Special Publications* (Eds J.M. Ole and D. Tom), **Volume 10**, pp. 211-232. Elsevier.

Smelror, M., Petrov, O., Larssen, G.B. and Werner, S. (2009) Geological history of the Barents Sea. *Norges Geol. undersøkelse***,** 1-135.

Surlyk, F. (1984) Fan-delta to submarine fan conglomerates of the Volgian-Valanginian Wollaston forland group, east Greenland.

Øvrebø, O. and Talleraas, E. (1977) The Structural geology of the Troms Area (Barents-Sea). *GeoJournal*, **1,** 47-54.

Appendix

MN87-501	T-016-85	T-89-405
MN87-502	T-018-85	T-89-406
MN87-505	T-025-85	T-89-407
MN87-507	T-026-85	T-89-408
MN87-508	T-03-84	T-89-409
MN87-509	T-034-85	T-89-410
MN87-511	T-035-85	T-89-413
NH9703-212M	T-036-85	TGS-90-201B
NH9703-9	T-04-84	TGS-90-202
NH9703R99-455	T-047-85	TGS-90-204
SG9714-406	T-06-84	TGS-90-405
T-007-85	T-09-84	TGS-90-406
T-009-85	T-5-83	TGS-90-407
T-01-84	T-6-83	TGS-90-409
T-010-85	T-89-201	TGS-90-411
T-011-85	T-89-203	TGS-90-412
T-012-85	T-89-204	TR73R1-101
T-013-85	T-89-205	TR73R1-711
T-014-85	T-89-206	NA-94-3D

Appendix 1, complete list of seimsic surveys/lines used in this study.

Appendix 2, complete image of the cored interval of the Knurr Formation in well 7019/1-1. Top of core (2220.0m TVD) is top left, bottom of the core (2234.3m TVD) is bottom right. Parts of the core is missing due to seal peal or sampling.

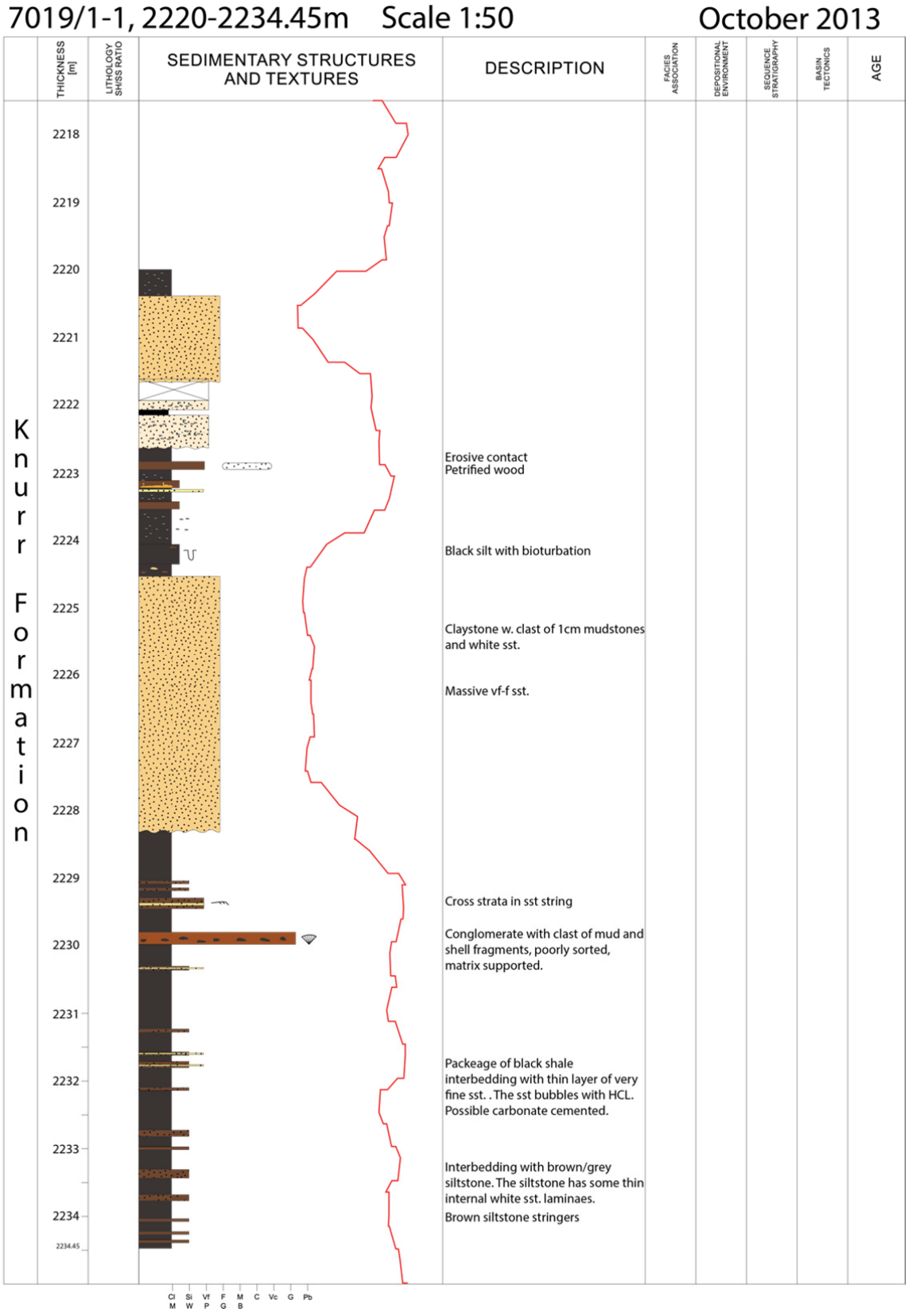

Appendix 3, complete lithological log of core 1, 7019/1-1 with comments.